# Chapter 10
# Ride Comfort and Road Holding


Real roads are far from flat. Even freshly paved highways have small imperfections that interact with the vehicle dynamics by exciting vehicle vertical vibrations.

The capability to smooth down road imperfections affects both the *comfort* and the *road holding* of the vehicle. Improving comfort means, basically, limiting the vertical acceleration fluctuations of the vehicle body and hence of passengers. Improving road holding means, among other things, limiting the fluctuations of the vertical force that each tire exchanges with the road.[1] The main parameters that affect both comfort and road holding are the suspension *stiffness* and *damping*.

The study of the vibrational behavior of a vehicle going straight at constant speed on a *bumpy road* is called *ride* [1, 3, 5, 6, 9, 11]. More precisely, ride deals with frequencies in the range 0.25–25 Hz for road cars, a bit higher for race cars. Tires can, among other things, absorb small road irregularities at high frequency because of their vertical elasticity and low mass. However, for frequencies below 3 Hz the tires have little influence and can be considered as rigid. Therefore, the burden to absorb bigger bumps goes to the vehicle suspensions.

While when studying the handling of a vehicle we were also interested in the suspension geometry, we focus here on *springs* and *dampers*. We look for criteria for selecting the right stiffness and the right amount of damping for each suspension.

Actually, this is only half the truth. Real suspensions have nonlinear springs and nonlinear dampers, whose features cannot be reduced to a single number like in the linear case. However, suspensions with linear behavior are a good introduction to the study of ride and road holding.

Although standard suspension systems are based on two components—springs and dampers (shock absorbers)—there is a third component that can turn out to be

[1] Of course, we mean fluctuations due to road imperfections, not to load transfers.

The original version of this chapter was revised: Belated corrections have been incorporated. The correction to this chapter is available at https://doi.org/10.1007/978-3-319-73220-6_12



M. Guiggiani, *The Science of Vehicle Dynamics*,
https://doi.org/10.1007/978-3-319-73220-6_10

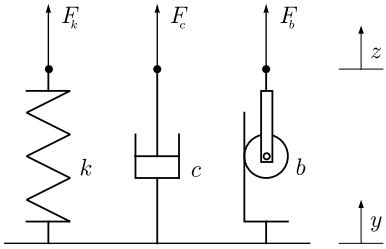


**Fig. 10.1** Schematics for spring, damper and inerter

useful in some cases. It is the so-called *inerter*. The inerter is a device that provides a force proportional to the relative *acceleration* between its attachment points, much like a linear damper provides a force proportional to the relative velocity and a linear spring a force proportional to the relative displacement (Fig. 10.1)

$$\begin{aligned} F_k &= k(z-y) \\ F_c &= c(\dot{z}-\dot{y}) \\ F_b &= b(\ddot{z}-\ddot{y}) \end{aligned} \tag{10.1}$$

The inerter was missing indeed, till quite recently [10]. A typical inerter incorporates a flywheel which rotates in proportion to the relative displacement between its two ends. So far, it has been employed in some Formula cars. We will show how it can improve, in some cases, the car road holding.

## 10.1 Vehicle Models for Ride and Road Holding

We are mostly interested in the vehicle vertical motion. To keep our ride analysis quite simple, we assume that the vehicle goes *straight* and at *constant speed*. Therefore, there are no handling and/or performance implications here. The ride analysis comes into play because of the *uneven road*. Actually, we ask for a very peculiar road, albeit uneven. It must have exactly the same profile for both wheels of the same axle, thus not inducing roll motion at all. That means that we can rely on a two-dimensional model.

The vehicle models set up for handling and performance are not suitable for ride. We need to develop a tailored model like, e.g., the four-degree-of-freedom model shown in Fig. 10.2. In this model there are three rigid bodies:

- the sprung mass $m_s$ (with moment of inertia $J_y$ w.r.t. its center of gravity $G_s$), which has vertical motion $z_s$ and pitch motion $\theta$;
- the front unsprung mass $m_{n_1}$, which has only vertical (hop) motion $y_1$;
- the rear unsprung mass $m_{n_2}$, which has only vertical (hop) motion $y_2$.

Also shown in Fig. 10.2 are the two suspension springs, with stiffnesses $k_1$ and $k_2$, and two dampers, with damping coefficients $c_1$ and $c_2$, along with two springs

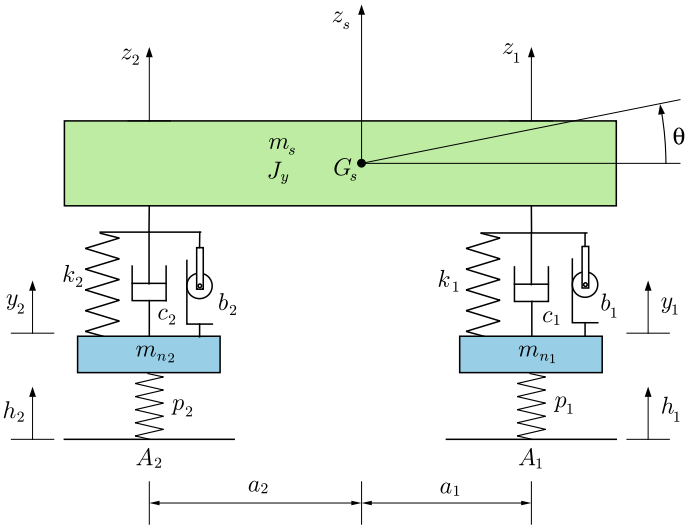


**Fig. 10.2** Four-degree-of-freedom model to study ride and road holding

$p_1$ and $p_2$ to model the tire vertical stiffnesses. Again, to keep the analysis simple, we assume that all these components have *linear* behavior. This is a very unrealistic hypothesis since real suspensions are designed to have hardening stiffness and are equipped with dampers with more resistance during the extension cycle than the compression cycle.

Inerters, with inertances $b_1$ and $b_2$, are also shown in Fig. 10.2. They have been used sparingly and only in some race cars. They are included for greater generality.

The vehicle model shown in Fig. 10.2 has four degrees of freedom. Points $A_1$ and $A_2$ are the centers of the front axle contact patches and of the rear axle contact patches, respectively. The two functions $h_1(t)$ and $h_2(t)$ are the road profiles as "felt" by the car, that is through the tires [4].

The sprung mass has two degrees of freedom $z_s$ and $\theta$. Alternatively, we could use, e.g., the vertical displacements $z_1$ and $z_2$. All displacements and rotations are absolute and taken from the static equilibrium position of the vehicle. We are investigating the oscillations with respect to the equilibrium position, that is the configuration the vehicle would have on a perfectly flat road.

The vehicle model shown in Fig. 10.2 is governed by three sets of equations, as usual:

1. congruence equations:

$$\begin{aligned} z_1 &= z_s + a_1\,\theta \\ z_2 &= z_s - a_2\,\theta \end{aligned} \tag{10.2}$$

that is a purely geometrical link between coordinates;

2. equilibrium equations:

$$\begin{aligned} m_s\ddot{z}_s &= F_1 + F_2 \\ J_y\ddot{\theta} &= F_1 a_1 - F_2 a_2 \\ m_{n_1}\ddot{y}_1 &= N_1 - F_1 \\ m_{n_2}\ddot{y}_2 &= N_2 - F_2 \end{aligned} \tag{10.3}$$

that is a link between forces or couples and accelerations;

3. constitutive equations:

$$\begin{aligned} F_1 &= -k_1(z_1 - y_1) - c_1(\dot{z}_1 - \dot{y}_1) - b_1(\ddot{z}_1 - \ddot{y}_1) = -(F_{k_1} + F_{c_1} + F_{b_1}) \\ F_2 &= -k_2(z_2 - y_2) - c_2(\dot{z}_2 - \dot{y}_2) - b_2(\ddot{z}_2 - \ddot{y}_2) = -(F_{k_2} + F_{c_2} + F_{b_2}) \\ N_1 &= -p_1(y_1 - h_1) \\ N_2 &= -p_2(y_2 - h_2) \end{aligned} \tag{10.4}$$

which model springs, dampers and inerters.

By $F_1$ and $F_2$ we mean the vertical forces exchanged between the sprung mass and the two unsprung masses, respectively. By $N_1$ and $N_2$ we mean the forces exchanged by each axle with the road. All forces must be intended as perturbations with respect to the static equilibrium position. That is why the weight was not included in the equations.

Combining the above sets of equations, we end up with a system of four linear differential equations with constant coefficients. They are the governing equations of this vehicle model

$$\mathbf{M}\,\ddot{\mathbf{w}} + \mathbf{C}\,\dot{\mathbf{w}} + \mathbf{K}\,\mathbf{w} = \mathbf{h} \tag{10.5}$$

where $\mathbf{w} = \mathbf{w}(t) = \big(z_s(t),\, \theta(t),\, y_1(t),\, y_2(t)\big)$ is the coordinate vector, and $\mathbf{h} = \mathbf{h}(t) = \big(0,\, 0,\, p_1 h_1(t),\, p_2 h_2(t)\big)$ is the road excitation. We also have the mass matrix$\mathbf{M}$

$$\mathbf{M} = \mathbf{M}_m + \mathbf{M}_b = \begin{bmatrix} m_s & 0 & 0 & 0 \\ 0 & J_y & 0 & 0 \\ 0 & 0 & m_{n_1} & 0 \\ 0 & 0 & 0 & m_{n_2} \end{bmatrix} + \begin{bmatrix} b_1 + b_2 & b_1 a_1 - b_2 a_2 & -b_1 & -b_2 \\ b_1 a_1 - b_2 a_2 & b_1 a_1^2 + b_2 a_2^2 & -b_1 a_1 & b_2 a_2 \\ -b_1 & -b_1 a_1 & b_1 & 0 \\ -b_2 & b_2 a_2 & 0 & b_2 \end{bmatrix} \tag{10.6}$$

the damping matrix $\mathbf{C}$

$$\mathbf{C} = \begin{bmatrix} c_1 + c_2 & c_1 a_1 - c_2 a_2 & -c_1 & -c_2 \\ c_1 a_1 - c_2 a_2 & c_1 a_1^2 + c_2 a_2^2 & -c_1 a_1 & c_2 a_2 \\ -c_1 & -c_1 a_1 & c_1 & 0 \\ -c_2 & c_2 a_2 & 0 & c_2 \end{bmatrix} \tag{10.7}$$

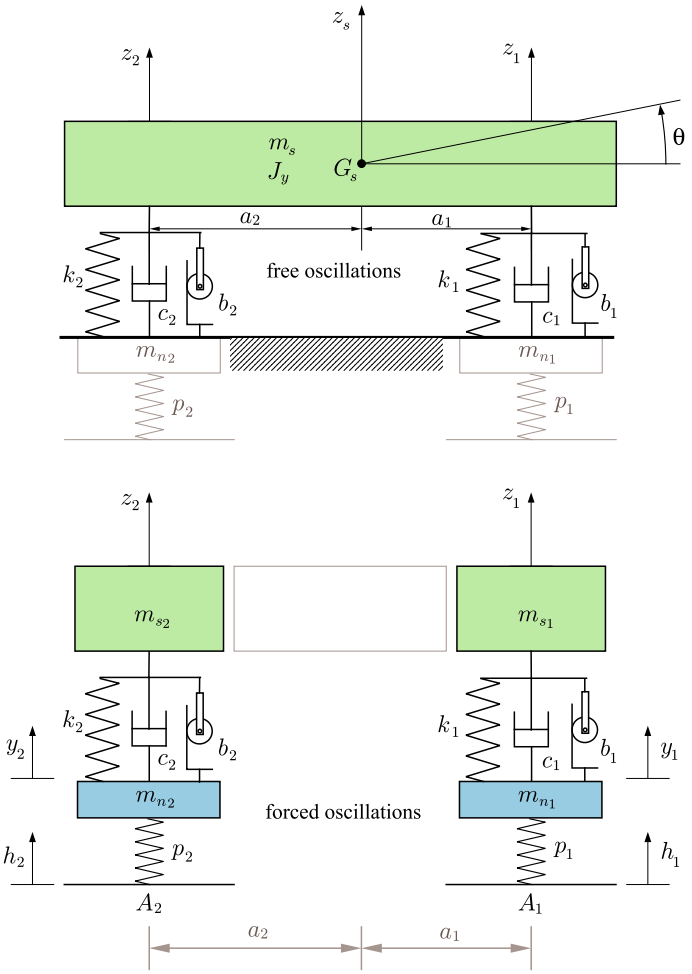


**Fig. 10.3** "Extraction" of two-degree-of-freedom models to study free vibrations (top) and forced vibrations (bottom). Gray lines show the dropped parts

and the stiffness matrix $\mathbf{K}$

$$\mathbf{K} = \mathbf{K}_k + \mathbf{K}_p = \begin{bmatrix} k_1 + k_2 & k_1 a_1 - k_2 a_2 & -k_1 & -k_2 \\ k_1 a_1 - k_2 a_2 & k_1 a_1^2 + k_2 a_2^2 & -k_1 a_1 & k_2 a_2 \\ -k_1 & -k_1 a_1 & k_1 & 0 \\ -k_2 & k_2 a_2 & 0 & k_2 \end{bmatrix} + \begin{bmatrix} 0 & 0 & 0 & 0 \\ 0 & 0 & 0 & 0 \\ 0 & 0 & p_1 & 0 \\ 0 & 0 & 0 & p_2 \end{bmatrix} \tag{10.8}$$

A linear four-degree-of-freedom system is quite simple in principle, but also quite cumbersome to be dealt with analytically without the aid of a computer. Therefore,

for educational purposes, it is useful to simplify this model further. The basic idea is to extract two models, both with two degrees of freedom. One model to study free vibrations and the other model to study forced vibrations. The two models are virtually obtained by cutting off the unnecessary parts (gray lines in Fig. 10.3) from the four-degree-of-freedom system.

The sprung mass $m_s$ is always much higher than the total unsprung mass $m_n = m_{n_1} + m_{n_2}$. Typically we have $m_s \simeq 10 m_n$. Moreover, tire stiffness is, except in Formula cars, much higher than the suspension stiffness. Typically, $p_i = 6 - 12\, k_i$. Therefore, the tires have little influence on the free vibrations and can be considered as rigid, as done in Fig. 10.3 (top). In Formula cars we have $p_i = 1 - 2\, k_i$.

On the other hand, the road disturbances involve also high frequencies, and tire stiffness has to be taken into account. For studying forced vibrations, the vehicle is then split into two half-car models, as in Fig. 10.3 (bottom), where

$$m_{s_1} = m_s \frac{a_2}{l} \qquad \text{and} \qquad m_{s_2} = m_s \frac{a_1}{l} \tag{10.9}$$

Instead of the half-car model, it is customary to use the *quarter car model*, which is like the half-car model with all quantities divided by two.

Both models are rather crude approximations, but nevertheless they can provide very useful insights on how to choose the springs and dampers (and, just in case, the inerters as well).

## 10.2 Quarter Car Model

The quarter car model is shown in Fig. 10.4. For simplicity we dropped the subscript in all quantities. The model consists of a sprung mass $m_s$ connected via the primary suspension to the unsprung mass $m_n$ of the axle. The suspension is supposed to have linear behavior with stiffness $k$ and damping coefficient $c$. An inerter, with inertance $b$, is also included. The tire vertical elasticity is represented again by a linear spring $p$. The tire damping is so small that it can be neglected.

Quite contrary to common practice, here we prefer not to split the car into four corners. Instead, we retain the sprung mass of the whole vehicle as $m_s$. Consistently, we have to include in $k$ the stiffnesses of the four suspensions and so on. Following this approach has several advantages over the classical quarter car model:

- we deal with only one model instead of two (front and rear);
- we do not have to arbitrarily split the mass into front mass and rear mass;
- we are not tempted to use misleading concepts like the front/rear natural frequency.

Therefore, we are actually using a *full car model*. We still call it quarter car model just for the sake of uniformity with other books.

This quarter (full) car model is mainly used to study the vibrational behavior of the vehicle when travelling on an uneven road. Therefore, the lowermost part of $p$

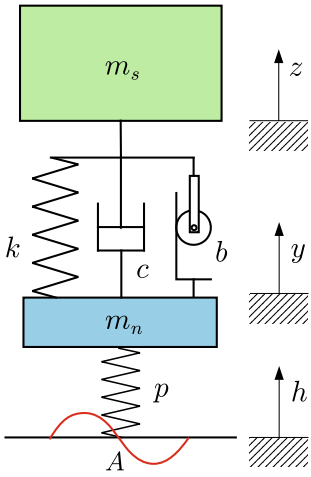


**Fig. 10.4** Quarter car model (better, full car model)

receives from the road a sinusoidal displacement $h(t) = H \cos \Omega t$. Someone may object that real roads are not sinusoidal in shape. However, any road profile $g(x)$ of length $L$ can be expressed by its Fourier series [4]

$$g(x) = \sum_{n=0}^{\infty} \left[ d_n \sin\left(\frac{2\pi n}{L} x\right) + e_n \cos\left(\frac{2\pi n}{L} x\right) \right], \tag{10.10}$$

that is as an infinite sum of trigonometric functions. Fortunately, it is possible to take only the first $n$ terms without missing too much information. If the vehicle travels with speed $u$, the Fourier term with spatial period $L/n$ acts as a forcing displacement of frequency $f_n = nu/L$. Therefore, the frequency of the excitation depends, obviously, on the speed of the vehicle.

Because of the assumed *linearity* of the quarter car model, we can take advantage of the *superposition principle*, and "feed" the system with one Fourier term at a time. Should the system be nonlinear, this trick would be meaningless and we could no longer apply a simple sinusoidal forcing function.

The quarter car model is a damped two-degree-of-freedom system. We employ as coordinates the vertical displacement $z$ of the sprung mass and the vertical displacement $y$ (hop) of the unsprung mass. The road surface vertical displacement $h(t)$ can be derived from the road surface profile and the car's speed. The equations of motion of the quarter car model are readily obtained from Fig. 10.4 (recommended), or as a special case of the equations given in Sect. 10.1

$$\begin{aligned} m_s \ddot{z} &= -b(\ddot{z} - \ddot{y}) - c(\dot{z} - \dot{y}) - k(z - y) \\ m_n \ddot{y} &= -b(\ddot{y} - \ddot{z}) - c(\dot{y} - \dot{z}) - k(y - z) - p(y - h) \end{aligned} \tag{10.11}$$

where, as already stated, $h(t) = H \cos \Omega t$ is the excitation due to the road asperities. The same equations in matrix notation become

$$\mathbf{M}\,\ddot{\mathbf{w}} + \mathbf{C}\,\dot{\mathbf{w}} + \mathbf{K}\,\mathbf{w} = \mathbf{h} \tag{10.12}$$

with mass matrix $\mathbf{M}$

$$\mathbf{M} = \mathbf{M}_m + \mathbf{M}_b = \begin{bmatrix} m_s & 0 \\ 0 & m_n \end{bmatrix} + \begin{bmatrix} b & -b \\ -b & b \end{bmatrix} = \begin{bmatrix} m_s + b & -b \\ -b & m_n + b \end{bmatrix} \tag{10.13}$$

damping matrix $\mathbf{C}$

$$\mathbf{C} = \begin{bmatrix} c & -c \\ -c & c \end{bmatrix} \tag{10.14}$$

and stiffness matrix $\mathbf{K}$

$$\mathbf{K} = \mathbf{K}_k + \mathbf{K}_p = \begin{bmatrix} k & -k \\ -k & k \end{bmatrix} + \begin{bmatrix} 0 & 0 \\ 0 & p \end{bmatrix} = \begin{bmatrix} k & -k \\ -k & k + p \end{bmatrix} \tag{10.15}$$

We are mainly interested in the steady-state response, that is in the particular integral of the system of differential equations (10.11). In a case like this, it can be expressed as

$$\begin{aligned} z(t) &= Z \cos(\Omega\, t + \varphi) \\ y(t) &= Y \cos(\Omega\, t + \psi) \end{aligned} \tag{10.16}$$

that is in oscillations with the same angular frequency $\Omega$ of the excitation, but also with nonzero phases $\varphi$ and $\psi$.

The mathematical analysis is much simpler if complex numbers are employed. The forcing function is therefore given as

$$h(t) = H(\cos \Omega t + i \sin \Omega t) = H \mathrm{e}^{i\Omega t} \tag{10.17}$$

with $H \in \mathbb{R}$. The steady-state solution is

$$\begin{aligned} z(t) &= Z\,[\cos(\Omega t + \varphi) + i \sin(\Omega t + \varphi)] = Z \mathrm{e}^{i(\Omega t + \varphi)} = Z \mathrm{e}^{i\varphi} \mathrm{e}^{i\Omega t} = \mathsf{Z} \mathrm{e}^{i\Omega t} \\ y(t) &= Y\,[\cos(\Omega t + \psi) + i \sin(\Omega t + \psi)] = Y \mathrm{e}^{i(\Omega t + \psi)} = Y \mathrm{e}^{i\psi} \mathrm{e}^{i\Omega t} = \mathsf{Y} \mathrm{e}^{i\Omega t} \end{aligned} \tag{10.18}$$

where $\mathsf{Z} = Z \mathrm{e}^{i\varphi}$ and $\mathsf{Y} = Y \mathrm{e}^{i\psi}$ are complex numbers with modulus $Z$ and $Y$, and phases $\varphi$ and $\psi$.

Inserting these expressions into (10.11) and dropping $\mathrm{e}^{i\Omega t}$ provides the following algebraic system of equations in the complex unknowns $\mathsf{Z}$ and $\mathsf{Y}$

$$\begin{cases} [(k - b\Omega^2) - m_s\Omega^2 + i\,c\,\Omega]\,\mathsf{Z} - [(k - b\Omega^2) + i\,c\,\Omega]\,\mathsf{Y} & = 0 \\ -[(k - b\Omega^2) + i\,c\,\Omega]\,\mathsf{Z} + [p + (k - b\Omega^2) - m_n\Omega^2 + i\,c\,\Omega]\,\mathsf{Y} & = pH \end{cases} \tag{10.19}$$

whose solution is

$$\begin{aligned} \frac{\mathsf{Z}}{H} &= \frac{p\,[(k - b\Omega^2) + i\,c\,\Omega]}{[(k - b\Omega^2) - m_s\Omega^2 + i\,c\,\Omega][p + (k - b\Omega^2) - m_n\Omega^2 + i\,c\,\Omega] - [(k - b\Omega^2) + i\,c\,\Omega]^2} \\ &= p\,\frac{[(k - b\Omega^2) + i\,c\,\Omega]}{d(\Omega^2) + i\,c\,\Omega\,e(\Omega^2)} = \mathsf{G}_z(\Omega) \end{aligned} \tag{10.20}$$

and

$$\frac{\mathsf{Y}}{H} = p\,\frac{[(k - b\Omega^2) - m_s\Omega^2 + i\,c\,\Omega]}{d(\Omega^2) + i\,c\,\Omega\,e(\Omega^2)} = \mathsf{G}_y(\Omega) \tag{10.21}$$

where, for compactness,

$$\begin{aligned} d(\Omega^2) &= m_s m_n \Omega^4 - \{[p + (k - b\Omega^2)]m_s + (k - b\Omega^2)\,m_n\}\Omega^2 + p(k - b\Omega^2). \\ e(\Omega^2) &= p - (m_s + m_n)\Omega^2 \end{aligned} \tag{10.22}$$

The non-dimensional complex functions $\mathsf{G}_z(\Omega)$ and $\mathsf{G}_y(\Omega)$, given in (10.20) and (10.21), can be directly employed to obtain the steady-state solution

$$\begin{aligned} z(t) &= H\,\mathsf{G}_z(\Omega)\mathrm{e}^{i\Omega t} \\ y(t) &= H\,\mathsf{G}_y(\Omega)\mathrm{e}^{i\Omega t} \end{aligned} \tag{10.23}$$

From a practical point of view, we are mostly interested in the *amplitude* of these oscillations as functions of $\Omega$

$$\frac{Z}{H} = \frac{|\mathsf{Z}|}{H} = p\sqrt{\frac{(k - b\Omega^2)^2 + c^2\Omega^2}{d^2(\Omega^2) + c^2\Omega^2\,e^2(\Omega^2)}} = |\mathsf{G}_z(\Omega)| \tag{10.24}$$

$$\frac{Y}{H} = \frac{|\mathsf{Y}|}{H} = p\sqrt{\frac{[(k - b\Omega^2) - m_s\Omega^2]^2 + c^2\Omega^2}{d^2(\Omega^2) + c^2\Omega^2\,e^2(\Omega^2)}} = |\mathsf{G}_y(\Omega)| \tag{10.25}$$

However, the phases can be obtained as well

$$\tan\varphi = \frac{\mathrm{Im}(\mathsf{Z})}{\mathrm{Re}(\mathsf{Z})} \qquad \tan\psi = \frac{\mathrm{Im}(\mathsf{Y})}{\mathrm{Re}(\mathsf{Y})} \tag{10.26}$$

The amplitude of the vertical accelerations of the sprung and unsprung masses are given by $\Omega^2 Z$ and $\Omega^2 Y$, respectively.

Due to the oscillations, there are fluctuations in the vertical force exchanged by the tires with the road. More precisely, we have a sinusoidal force $\mathsf{N}\mathrm{e}^{i\Omega t}$ superimposed

on the constant force due to weight and, possibly, to aerodynamic downforces. From the quarter (full) car model of Fig 10.4 we get

$$\mathsf{N}e^{i\Omega t} = p(h-y) = p(H-\mathsf{Y})e^{i\Omega t} \tag{10.27}$$

From (10.21), we obtain the amplitude $N$ as a function of the angular frequency $\Omega$

$$\begin{aligned}\frac{N}{p\,H} = \frac{|\mathsf{N}|}{p\,H} &= \left|\frac{m_s m_n \Omega^4 - (m_s+m_n)\Omega^2[(k-b\Omega^2)+i\,c\,\Omega]}{d(\Omega^2)+i\,c\,\Omega\,e(\Omega^2)}\right| \\ &= \Omega^2\sqrt{\frac{[m_s m_n\Omega^2-(k-b\Omega^2)(m_s+m_n)]^2+c^2\Omega^2(m_s+m_n)^2}{d^2(\Omega^2)+c^2\Omega^2\,e^2(\Omega^2)}}\end{aligned} \tag{10.28}$$

### 10.2.1 The Inerter as a Spring Softener

It is worth noting that all these expressions include the term $k-b\Omega^2$. This is the key to understand the *inerter* (also called J-Damper). It is pretty much like having a system whose suspension stiffness is sensitive to the frequency $\Omega$ of the excitation. At low frequencies $k-b\Omega^2 \simeq k$, but at high frequencies $k-b\Omega^2 \ll k$. The inertance $b$ acts as a *spring softener*. This is a very interesting feature in Formula cars, with high aerodynamic loads, because we can use very stiff springs, thus limiting the spring deflection due to variable aerodynamic downforces, but at the same time the car will be able to absorb the high frequency road asperities, as if it were equipped with not-so-stiff springs. We will elaborate this idea quantitatively and in more detail in Sect. 10.3.3.

### 10.2.2 Quarter Car Natural Frequencies and Modes

A linear two-degree-of-freedom vibrating system, damped or not, has two natural modes, each one associated with its natural frequency.

To obtain these two modes, we consider the homogeneous counterpart of the system of differential equations (10.12)

$$\mathbf{M}\,\ddot{\mathbf{w}}_o + \mathbf{C}\,\dot{\mathbf{w}}_o + \mathbf{K}\,\mathbf{w}_o = \mathbf{0} \tag{10.29}$$

We seek a solution like

$$\mathbf{w}_o = \mathbf{x}e^{\mu t} \tag{10.30}$$

which, when inserted into (10.29), yields

$$e^{\mu t}(\mu^2\mathbf{M}+\mu\mathbf{C}+\mathbf{K})\mathbf{x} = \mathbf{0} \tag{10.31}$$

The four values of $\mu$ that make (10.30) truly a solution are the roots of the characteristic equation

$$\det(\mu^2\mathbf{M} + \mu\mathbf{C} + \mathbf{K}) = 0 \tag{10.32}$$

In an underdamped vibrating system, the four $\mu$ are complex numbers, complex conjugates in pairs

$$\begin{aligned} \mu_1 &= -\zeta_1\omega_1 + i\omega_1\sqrt{1-\zeta_1^2} \qquad \mu_3 = \bar{\mu}_1 = -\zeta_1\omega_1 - i\omega_1\sqrt{1-\zeta_1^2} \\ \mu_2 &= -\zeta_2\omega_2 + i\omega_2\sqrt{1-\zeta_2^2} \qquad \mu_4 = \bar{\mu}_2 = -\zeta_2\omega_2 - i\omega_2\sqrt{1-\zeta_2^2} \end{aligned} \tag{10.33}$$

where $0 \le \zeta_i < 1$ are the damping ratios (or damping factors), and $\omega_i$ are close to the natural angular frequencies $\omega_{u_i}$ of the undamped system.[2] The two natural angular frequencies of the *damped* system (i.e., of the quarter car model) are

$$\omega_{d_i} = \omega_i\sqrt{1-\zeta_i^2} \tag{10.34}$$

Once the four $\mu_i$ have been obtained, we can go back to (10.31) and obtain the corresponding generalized eigenvectors $\mathbf{x}_i \in \mathbb{C}^2$, again complex conjugates in pairs. The general solution of (10.29) is given as linear combination of complex exponential functions

$$\begin{aligned} \mathbf{w}_o(t) = {} & \gamma_1\mathbf{x}_1 e^{(-\zeta_1\omega_1 + i\omega_{d_1})t} + \bar{\gamma}_1\bar{\mathbf{x}}_1 e^{(-\zeta_1\omega_1 - i\omega_{d_1})t} \\ & + \gamma_2\mathbf{x}_2 e^{(-\zeta_2\omega_2 + i\omega_{d_2})t} + \bar{\gamma}_1\bar{\mathbf{x}}_2 e^{(-\zeta_2\omega_2 - i\omega_{d_2})t} \end{aligned} \tag{10.35}$$

As an introduction to the general case, it is useful to study first two very special cases, that is $c = 0$ and $c = \infty$.

#### 10.2.2.1 Undamped Quarter Car Model

Setting $c = 0$ makes the quarter car model a completely *undamped* two-degree-of-freedom vibrating system.

According to the expression of $d(\omega^2)$ in (10.22), the two natural angular frequencies $\omega_{u_1}$ and $\omega_{u_2}$ of the undamped system are the solutions of the algebraic equation

$$m_s m_n\omega^4 - \{[p + (k - b\omega^2)]m_s + (k - b\omega^2)\, m_n\}\omega^2 + p\,k = 0 \tag{10.36}$$

that is

[2] Let $\omega_{u_1} < \omega_{u_2}$, then $\omega_{u_1} < \omega_1$ and $\omega_2 < \omega_{u_2}$. Moreover, $\omega_{u_1}\omega_{u_2} = \omega_1\omega_2$.

$$\omega_{u_{1,2}}^2 = \frac{k(m_n + m_s) + (b + m_s)p}{2m_n m_s + 2b(m_n + m_s)} \pm \frac{\sqrt{-4k[m_n m_s + b(m_n + m_s)]p + [k(m_n + m_s) + (b + m_s)p]^2}}{2m_n m_s + 2b(m_n + m_s)} \tag{10.37}$$

which, if there is no inerter $b$, simplifies into

$$\begin{aligned} \omega_{u_{1,2}}^2 &= \frac{k(m_n + m_s) + m_s p \pm \sqrt{-4k(m_n m_s)p + [k(m_n + m_s) + m_s p]^2}}{2m_n m_s} \\ &= \frac{1}{2}\left[\frac{p + k}{m_n} + \frac{k}{m_s} \pm \sqrt{\left(\frac{p + k}{m_n} - \frac{k}{m_s}\right)^2 + \frac{4k^2}{m_n m_s}}\right] \end{aligned} \tag{10.38}$$

As already stated, in all road cars we have $m_s \gg m_n$ and $p \gg k$. Therefore, we can take the first-order Taylor expansion approximation of (10.38) for small values of $m_n$ and $k$

$$\omega_{u_1}^2 \simeq \frac{kp}{(p + k)m_s} \quad \text{and} \quad \omega_{u_2}^2 \simeq \frac{p + k}{m_n} \tag{10.39}$$

In most cases, this very simple formulæ provide very accurate estimates of the natural frequencies of the undamped quarter car model. For instance, with the data reported in the caption of Fig. 10.7, we get the following values using first the exact formula and then the approximate one

$$\begin{aligned} f_{u_1} &= \frac{\omega_{u_1}}{2\pi} = 1.254 \text{ Hz} \simeq 1.255 \text{ Hz} \\ f_{u_2} &= \frac{\omega_{u_2}}{2\pi} = 12.64 \text{ Hz} \simeq 12.63 \text{ Hz} \end{aligned} \tag{10.40}$$

The results are almost identical. Typically, in road cars, $f_{u_2}/f_{u_1} \simeq 10$.

Of course there is a clear physical interpretation. The two approximate natural frequencies (10.39) would be the exact natural frequencies of the two one-degree-of-freedom systems shown in Fig. 10.5. Indeed, as also shown in Fig. 10.5, the two natural modes of the *undamped* quarter car model are very peculiar. For instance, again with the same data, the first mode, the one with $f_{u_1} = 1.2$ Hz, has $z(t) = 8.9y(t)$, whereas the second mode, with $f_{u_2} = 12.6$ Hz, has $z(t) = -y(t)/89$. That is, they look pretty much as if, in each mode, only one mass at the time were oscillating.

A Formula 1 car exhibits similar figures, although with some noteworthy differences. The undamped system has $f_{u_1} \simeq 5$ Hz with $z(t) = 2.5y(t)$, and $f_{u_2} \simeq 32$ Hz with $z(t) = -y(t)/25$.

It is very important to know that while the first natural mode is quite insensitive to damping, the second natural mode is very damping dependent. For instance, in a road car having what will be called the *optimal damping* $c_{\text{opt}}$, the first mode has $f_1 = 1.21$ Hz, which is very close to $f_{u_1} = 1.25$ Hz with no damping. Moreover, the amplitude of $z(t)$ is about 8.4 times the amplitude of $y(t)$, pretty much like in the

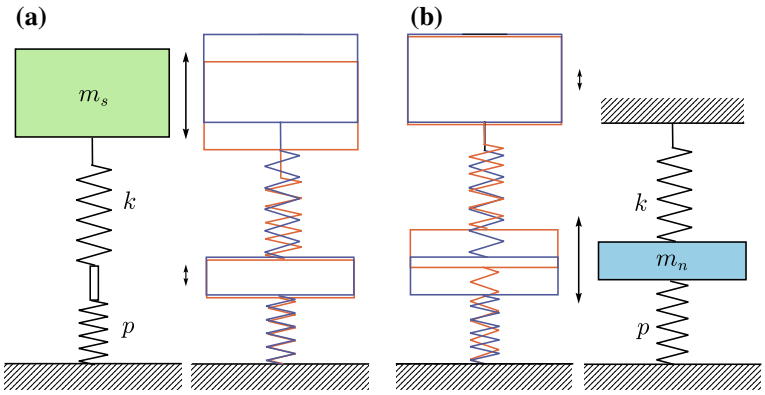


**Fig. 10.5** One-degree-of-freedom systems for the *approximate* evaluation of the two natural frequencies of the *undamped* quarter car model (road cars only)

undamped case. The second mode, on the other hand, has $f_{u_2} = 11.1\,\text{Hz}$ instead of $f_2 = 12.6\,\text{Hz}$ with no damping. But the most striking difference is that the amplitude of $y(t)$ is only about 12 times the amplitude of $z(t)$, instead of about 90 times, as it was with no damping. This is to say that we should not extrapolate results obtained with no damping to the real case, when there is a lot of damping because of the dampers.

#### 10.2.2.2 Quarter Car Model with Stuck Damper

The other theoretical case is $c = \infty$, pretty much like having a stuck damper. The system behaves like an undamped one-degree-of-freedom system with one mass $m_s + m_n$ on top of a spring $p$ (Fig. 10.6). There is only one natural frequency

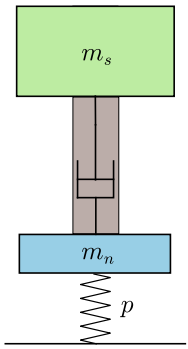


**Fig. 10.6** Quarter car model with stuck damper, that is with $c = \infty$

$$\omega_c = \sqrt{\frac{p}{(m_s + m_n)}} \tag{10.41}$$

At first, it may appear a bit strange that $c = \infty$ leads to an undamped system. The effect of such an high value of $c$ is to stick $m_s$ and $m_n$ together, thus leaving only the undamped oscillation with stiffness $p$.

## 10.3 Damper Tuning

The quarter car model can now be used as a tool for the selection of the damping coefficient $c$ of the damper. Of course, we have first to set up our goal. Typically, in road cars we are interested in minimizing the amplitude $\Omega^2 Z$ of the vertical acceleration $\ddot{z} = \Omega^2 \mathsf{Z} e^{i\Omega t}$ of the sprung mass, thus optimizing the passenger comfort. On the other hand, in race cars we are more interested in minimizing the amplitude $N$ of the oscillating part of the vertical force $\mathsf{N} e^{i\Omega t}$, thus improving road holding.

### *10.3.1 Optimal Damper for Comfort*

To select the right amount of damping to optimize passenger comfort, let us plot the normalized acceleration amplitude $\Omega^2 Z/H$ versus the angular frequency $\Omega$ of the road excitation. This is done in Fig. 10.7 for some values of $c$, including the

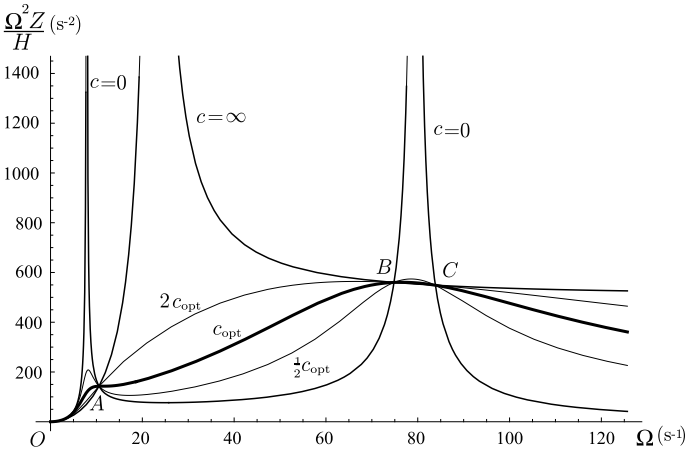


**Fig. 10.7** Amplitude of the vertical acceleration of the sprung mass in a typical road car ($m_s = 1000$ kg, $m_n = 100$ kg, $k = 70$ kN/m and $p = 560$ kN/m)

two extreme cases $c = 0$ and $c = \infty$. The figure was obtained with $m_s = 1000$ kg, $m_n = 100$ kg, $k = 70$ kN/m and $p = 560$ kN/m, that is with $m_s = 10m_n$ and $p = 8k$.

The plot for $c = 0$ and the plot for $c = \infty$ have four common points, marked by $O$, $A$, $B$ and $C$ in Fig. 10.7. Obviously, all other curves, for any value of $0 < c < \infty$, must pass through the same points.

The best curve, and hence the best value of the damping coefficient $c$, is perhaps the one with *horizontal tangent at point A*. It is a good compromise, as suggested in 1950 by Bourcier de Carbon [2]. As also shown in Fig. 10.7, lower or higher values of $c$ would yield less uniform curves.

To obtain this optimal value $c_{\text{opt}}$, we have to impose that the derivative at $A$ be zero

$$\left.\frac{\partial\left(\Omega^2 Z(c,\Omega)\right)}{\partial\Omega}\right|_{\Omega=\Omega_A} = 0 \tag{10.42}$$

where $Z = Z(c, \Omega)$ is given in (10.24). The result is the sought *optimal damping coefficient* $c_{\text{opt}}$

$$c_{\text{opt}} = \sqrt{\frac{m_s k}{2}}\sqrt{\frac{p+2k}{p}} \tag{10.43}$$

where the second square root is quite close to one. With the data used to draw Fig. 10.7 we get $c_{\text{opt}} = 5916.08 \times 1.118 = 6614.38$ Ns/m. With this value of the damping coefficient, we have that the two natural modes of the quarter car model have, respectively, $\zeta_1 = 0.34$ and $\omega_{d_1} = \omega_1\sqrt{1-\zeta_1^2} = 8.1$ rad/s for the first mode, and $\zeta_2 = 0.44$ and $\omega_{d_2} = \omega_2\sqrt{1-\zeta_2^2} = 77.0$ rad/s for the second mode. We see that both modes are underdamped ($\zeta_i < 1$), but with a far from negligible amount of damping. A vehicle engineer should always bear in mind that the damping ratio $\zeta_1$ of the first mode is usually something between 0.3 and 0.4 in road cars.

Another observation is in order here. Although the two values of $\zeta_i$ are quite similar, the time-rate decaying of the two modes, which depend on $\zeta_i\omega_i$, are drastically different because the two $\omega_i$ are quite far apart. For instance, in one second the amplitude of the first mode drops from 1 to $\mathrm{e}^{-0.34\times 8.61} = 0.05$, while that of the second mode drops to $\mathrm{e}^{-0.44\times 85.7} = 10^{-17}$. Quite a big difference.

It is worth noting that $c_{\text{opt}}$ does not depend on the unsprung mass $m_n$. Therefore, it is not necessary to change the dampers when, for instance, mounting light alloy wheel rims. On the other hand, stiffer springs do require harder dampers.

Saying that $m_n$ does not affect $c_{\text{opt}}$ does not imply that the unsprung mass has no influence at all. The comfort performances for three different values of the ratio $m_n/m_s$ are shown in Fig. 10.8. The lower the unsprung mass, the better, because the resulting curve is more uniform.

The formula for the optimal value of the damping coefficient here obtained perhaps works to get a close to optimal damping coefficient for a Formula 1 car as well. Figure 10.9 is the counterpart of Fig. 10.7. We see that the two Figures are quite different, but the $c_{\text{opt}}$ curve is probably the best.

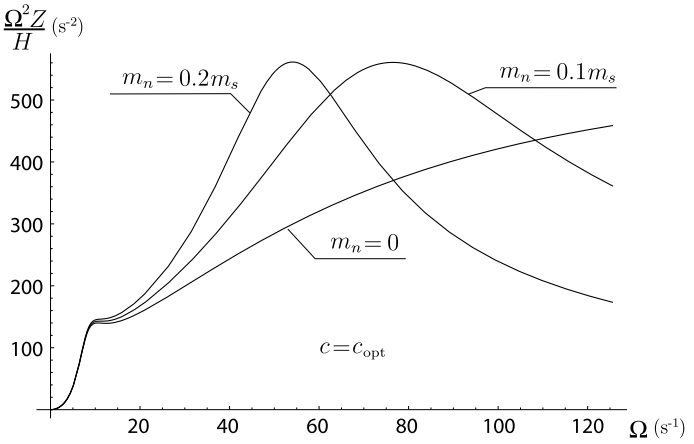


**Fig. 10.8** Amplitude of the vertical acceleration of the sprung mass for three values of the unsprung mass (road car with $m_s = 1000$ kg, $c = c_{\text{opt}}$, $k = 70$ kN/m and $p = 560$ kN/m)

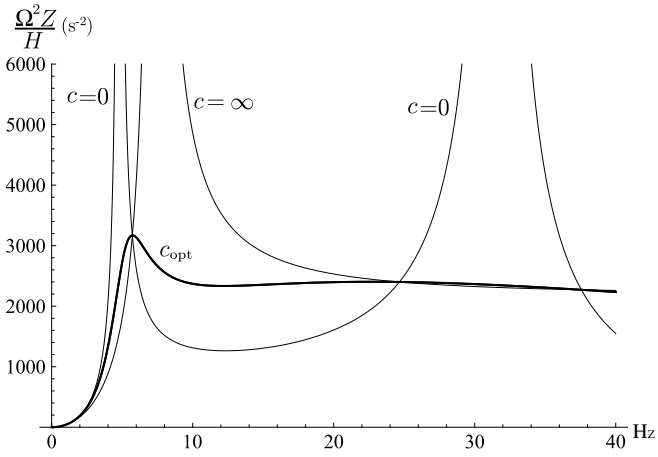


**Fig. 10.9** Amplitude of the vertical acceleration of the sprung mass in a typical Formula 1 car

### *10.3.2 Optimal Damper for Road Holding*

Needless to say that we need high vertical loads to have high friction forces. When the road is not flat, the vertical force fluctuations may impair road holding. Therefore, we are interested in how to determine the best damper tuning to counteract these force fluctuations as much as possible. The quarter car model can be usefully employed to this end. We have already obtained in (10.28) the expression of the amplitude of the sinusoidal component of the vertical load. Of course, it is superimposed on the vertical load due to weight, load transfers and, possibly, aerodynamic downforces.

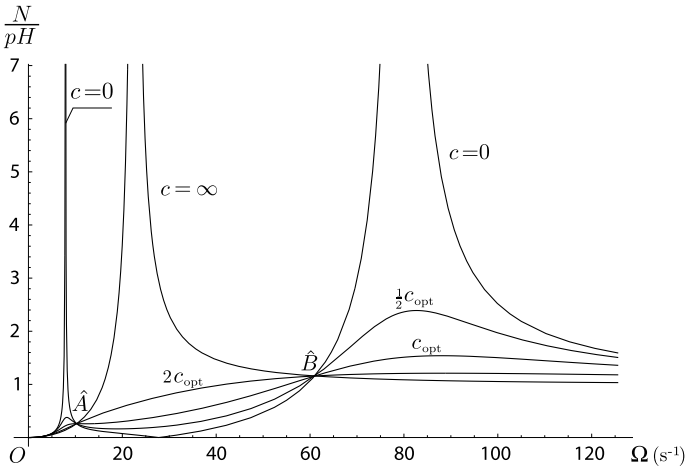


**Fig. 10.10** Amplitude of the sinusoidal vertical load for a road car ($m_s = 1000$ kg, $m_n = 100$ kg, $k = 70$ kN/m and $p = 560$ kN/m)

The plot of the normalized amplitude $N/(pH)$ versus $\Omega$ is shown in Fig. 10.10 for several values of the damping coefficient $c$. As before, there are the curves for the extreme cases $c = 0$ and $c = \infty$. In this case there are only three fixed points $O$, $\hat{A}$ and $\hat{B}$. The curve corresponding to $c = \frac{1}{2}c_{\text{opt}}, c_{\text{opt}}, 2\,c_{\text{opt}}$ are also shown in Fig. 10.10. As before, we have assumed $m_s = 1000$ kg, $m_n = 100$ kg, $k = 70$ kN/m and $p = 560$ kN/m, that is $m_s = 10m_n$ and $p = 8k$.

The curve for $c = c_{\text{opt}}$ is not as good as it was with respect to comfort. For road holding optimization in road cars, it is better to use higher values of the damping coefficient $c$, that is $c > c_{\text{opt}}$.

Reducing the unsprung masses is very beneficial for road holding, as shown in Fig. 10.11. We see that the lower the unsprung mass, the lower the vertical force amplitude, and hence the better the road holding. Therefore, using light alloy wheels is certainly a way to improve road holding.

### *10.3.3 The Inerter as a Tool for Road Holding Tuning*

Formula cars, and Formula 1 cars in particular, have aerodynamic devices that provide fairly high downforces at high speed. These devices are most efficient if kept at constant distance from the road surface. To reduce the spring deflections under variable aerodynamic loads, very stiff springs have to be used. However, stiff springs are not very good to absorb road irregularities. Here is where the *inerter* comes into play. It works as a sort of spring softener at high frequencies, while being almost irrelevant with respect to static or slowly varying loads.

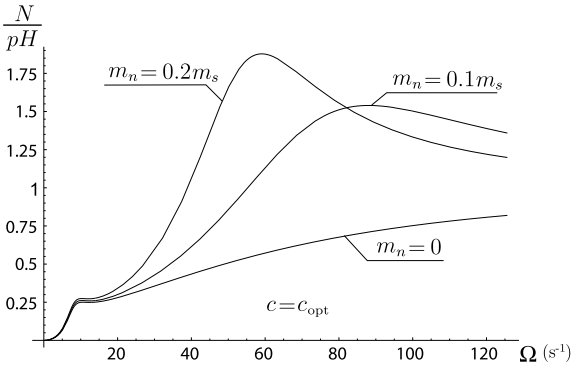


**Fig. 10.11** Amplitude of the sinusoidal vertical load for a road car for three values of the unsprung mass and $c = c_{\text{opt}}$

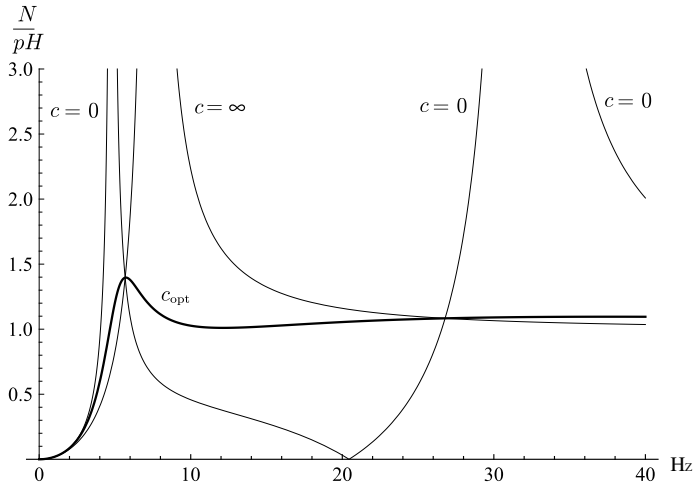


**Fig. 10.12** Amplitude of the sinusoidal vertical load for a typical Formula 1 car

Let us have a look at the counterpart of Fig. 10.10 for, e.g., a Formula 1 car. The plot of $N/(pH)$ versus $\Omega$ for a Formula 1 car is shown in Fig. 10.12. Interestingly enough, the value of $c_{\text{opt}}$ is optimal indeed. Any other value would be worse.

We are interested in increasing the spring stiffness $k$ without impairing the suspension capability to filter down road irregularities. Unfortunately, simply stiffening the springs brings a worse plot of $N/(pH)$, as shown in Fig. 10.13 (dashed line). However, the inerter can help in balancing the stiffer spring, and, in fact we end up with a much better plot (thick solid line in Fig. 10.13). Typically, we can increase the stiffness by 10–20%, with an inertance of 25–100 kg per wheel in a Formula Indy car.

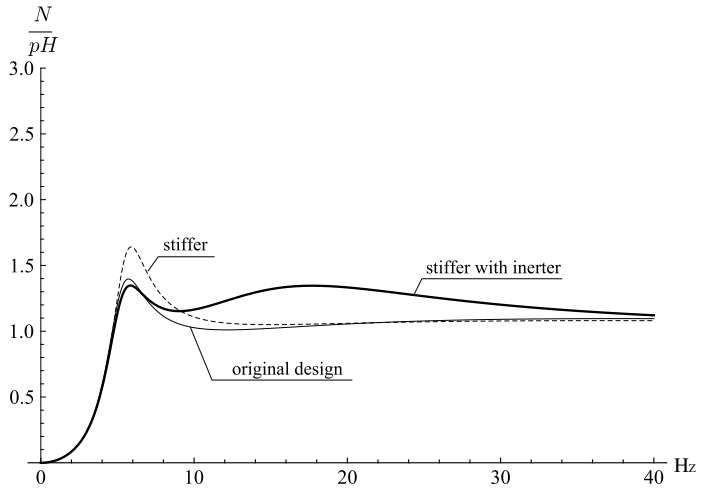


**Fig. 10.13** Beneficial effect of the inerter in a Formula 1 car with stiffer springs

It is worth noting that in ordinary road cars the inerter would not be beneficial. This is due to the totally different values of mass, stiffnesses, etc. Indeed, Figs. 10.10 and 10.12 are very different.

## 10.4 More General Suspension Layouts

More complex suspension layouts are possible. Some of them can be obtained by setting to zero some components in Fig. 10.14. Of course, never forget that dampers and inerters always need a spring in parallel to work properly.

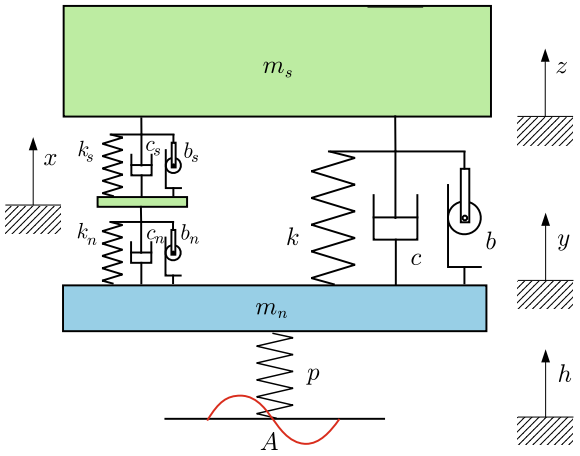


**Fig. 10.14** Quite general suspension scheme

It is kind of interesting to note that setting $c_s = b_n = 0$ is not equivalent to $c_n = b_s = 0$. Finding the optimal configuration is not an easy task, but could in some cases turns out to be very rewarding.

## 10.5 Road Profiles

In probability theory, stationary ergodic process is a random process which exhibits both stationarity and ergodicity. In essence this implies that the random process will not change its statistical properties with time and that its statistical properties (such as the theoretical mean and variance of the process) can be deduced from a single, sufficiently long sample of the process.

Road elevation profiles are stationary ergodic processes. This allows for fairly simple statistical treatment.

The Fourier transform $F(\omega)$ is a very powerful tool to obtain the frequency feature of a given function $f(x)$

$$F(\omega) = \int_{-\infty}^{+\infty} f(x)\mathrm{e}^{-i\omega x}\mathrm{d}x \tag{10.44}$$

The function $F(\omega) \in \mathbb{C}$ is precisely the frequency spectrum of $f(x)$.

We cannot apply directly the Fourier transform to a given road profile $g(x) \in \mathbb{R}$ because it does not tend to zero when $x \to \pm\infty$. However, we can introduce the spatial autocorrelation function $R_g(\tau)$ defined by

$$R_g(\tau) = \lim_{L\to\infty} \frac{1}{L} \int_{-L/2}^{+L/2} g(x)g(x+\tau)\mathrm{d}x \tag{10.45}$$

where $L$ is the length of the road with profile $g(x)$, and then compute its *power spectral density* (PSD) as its Fourier transform

$$S_g(s) = \int_{-\infty}^{+\infty} R(\tau)\mathrm{e}^{-is\tau}\mathrm{d}\tau \tag{10.46}$$

The power spectral density is measured in $\mathrm{m}^2$/(cycles/m), if $g$ is in meters and $s$ is in cycles/m. Therefore, $s$ is the spatial frequency.

If the vehicle travels at constant speed $u$, we can switch from the profile $g(x)$ to the time history $h(t)$ by means of the simple formula $h(t) = g(ut)$. The PSD $S_h(f)$, measured in m/Hz, of $h(t)$ can be obtained from $S_g(s)$ using

$$S_h(f) = \frac{S_g(f/u)}{u} \tag{10.47}$$

In general, if we know the PSD $S_h(f)$ of the excitation $h(t)$ and the frequency gain $\mathsf{G}_z(\Omega)$ of the linear system at hand, we can easily obtain the PSD of the system response $z(t)$ as

$$S_z(f) = |\mathsf{G}_z(2\pi f)|^2 S_h(f) \tag{10.48}$$

where, as well known, $\Omega = 2\pi f$.

For instance, the PSD $S_a(f)$ of the vertical acceleration $\ddot{z}$ of the sprung mass of the quarter car model is

$$S_a(f) = |(2\pi f)^2\, \mathsf{G}_z(2\pi f)|^2 S_h(f), \tag{10.49}$$

with $\mathsf{G}_z(\Omega) = \mathsf{G}_z(2\pi f)$ given in (10.20).

There is experimental evidence that the PSD of road profiles has a typical trend: the amplitude diminishes rapidly with the spatial frequency $s$. An often employed empirical formula for this behavior is

$$S_g(s) = Bs^{-k} \tag{10.50}$$

Unfortunately, there is not much agreement on the value of the exponent $k$. Typically it ranges between 2 and 4, including fractional values. The constant $B$ characterizes the roughness of the road profile. The smoother the profile, the lower $B$. It is worth noting that the units to measure $B$ are affected by the value of the exponent $k$.

According to (10.47), the counterpart of (10.50) in terms of time frequencies is

$$S_h(f) = Bu^{k-1} f^{-k} \tag{10.51}$$

which, obviously, shows that increasing the vehicle speed brings an increment in the PSD of the excitation.

## 10.6 Free Vibrations of Road Cars

The quarter car model looks at each axle as if it were alone. But it is not. Cars have two axles, and both take part in the vehicle body oscillations. Moreover, when we obtained the optimal value $c_{\text{opt}}$ of the damping coefficient in (10.43) by means of the quarter car model, that was a function of the suspension stiffness $k$, beside the sprung mass $m_s$ and the tire vertical stiffness $p$. But how was the stiffness $k$ set? We do not have much freedom about $m_s$ and $p$, and we may assume both of them as given for a certain kind of vehicle. But the stiffness $k$ can be selected quite freely, for both front and rear axles.

Free oscillations are what happens right after the car has hit an isolated bump or hole. Since road cars usually do not employ the inerter, we use the even simpler two-degree-of-freedom model shown in Fig. 10.15, instead of the model of Fig. 10.3. As already discussed, we can safely consider the tires as rigid. The tires are indeed

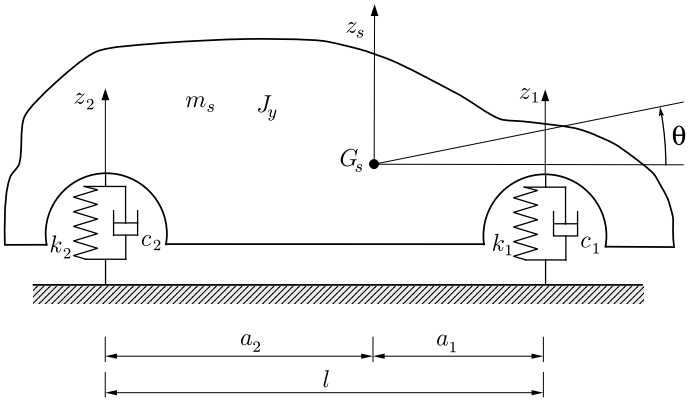


**Fig. 10.15** Two-degree-of-freedom system for bounce and pitch analysis (rigid tires)

much stiffer than the springs, and at low frequencies (1–2 Hz) the unsprung masses oscillate very little. Moreover, the mode with higher natural frequency decays almost instantaneously, as already shown.

The analysis of the model of Fig. 10.15 will provide useful hints for the selection and tuning of the front and rear stiffnesses $k_1$ and $k_2$.

### *10.6.1 Governing Equations*

To obtain all relevant equations for the two-degree-of-freedom vehicle model under investigation we follow the same path as in Sect. 10.1. We have (Fig. 10.15)

1. congruence equations:

$$\begin{aligned} z_1 &= z_s + a_1\,\theta \\ z_2 &= z_s - a_2\,\theta \end{aligned} \tag{10.52}$$

   that is a purely geometrical link between coordinates;
2. equilibrium equations:

$$\begin{aligned} m_s\ddot{z}_s &= F_1 + F_2 \\ J_y\ddot{\theta} &= F_1 a_1 - F_2 a_2 \end{aligned} \tag{10.53}$$

   that is a link between forces or couples and accelerations; and
3. constitutive equations:

$$\begin{aligned} F_1 &= -k_1 z_1 - c_1 \dot{z}_1 \\ F_2 &= -k_2 z_2 - c_2 \dot{z}_2 \end{aligned} \tag{10.54}$$

When combined all together, they provide the governing equations

$$\begin{aligned} m_s\ddot{z}_s &= -k_1(z_s + a_1\,\theta) - c_1(\dot{z}_s + a_1\,\dot{\theta}) - k_2(z_s - a_2\,\theta) - c_2(\dot{z}_s - a_2\,\dot{\theta}) \\ J_y\ddot{\theta} &= [-k_1(z_s + a_1\,\theta) - c_1(\dot{z}_s + a_1\,\dot{\theta})]a_1 - [-k_2(z_s - a_2\,\theta) - c_2(\dot{z}_s - a_2\,\dot{\theta})]a_2 \end{aligned} \tag{10.55}$$

that can also be written in matrix notation as

$$\mathbf{M}\,\ddot{\mathbf{w}}_o + \mathbf{C}\,\dot{\mathbf{w}}_o + \mathbf{K}\,\mathbf{w}_o = \mathbf{0} \tag{10.56}$$

where $\mathbf{w}_o = (z_s, \theta)$. Formally, they look like (10.5), except for being homogeneous now. The $2 \times 2$ matrices are

$$\mathbf{M} = \begin{bmatrix} m_s & 0 \\ 0 & J_y \end{bmatrix} \tag{10.57}$$

$$\mathbf{C} = \begin{bmatrix} c_1 + c_2 & c_1a_1 - c_2a_2 \\ c_1a_1 - c_2a_2 & c_1a_1^2 + c_2a_2^2 \end{bmatrix} \tag{10.58}$$

and

$$\mathbf{K} = \begin{bmatrix} k_1 + k_2 & k_1a_1 - k_2a_2 \\ k_1a_1 - k_2a_2 & k_1a_1^2 + k_2a_2^2 \end{bmatrix} \tag{10.59}$$

As well known, the solutions of (10.56) are in the form $\mathbf{w}_o(t) = \mathbf{x}\mathrm{e}^{\mu\,t}$, with $\mu$ and $\mathbf{x}$ such that

$$(\mu^2\mathbf{M} + \mu\mathbf{C} + \mathbf{K})\mathbf{x} = \mathbf{0} \tag{10.60}$$

Quite surprisingly, it is common practice in the vehicle dynamic community to discard damping when studying free oscillations of a vehicle. Most books do that. But why?

Actually, vehicles have a lot of damping (in the quarter car model we obtained damping ratios $\zeta_i$ in the range 0.3–0.5). Perhaps they are the most damped system in mechanical engineering, and a good engineer cannot discard something which is not negligible at all. A rationale for neglecting damping should be provided, as a minimum. Unfortunately, in most cases there is just a sentence stating that damping will be neglected.

Free oscillations of undamped systems are much more predictable than those of a general damped system. Moreover, through modal analysis they can be treated as a collection of single-degree-of-freedom oscillators. But, we insist, vehicles are not undamped. They are very damped systems.

Fortunately, there is a way to have a damped system behave pretty much like an undamped system: it must have *proportional damping* (also called Rayleigh damping). Modes of proportionally damped systems preserve the simplicity of the real normal modes as in the undamped case, as we are going to discuss in a while.

### 10.6.2 Proportional Viscous Damping

The definition of proportional viscous damping is (e.g., [8, p. 522])

$$\mathbf{C} = \alpha\,\mathbf{M} + \beta\,\mathbf{K} \tag{10.61}$$

that is the damping matrix must be a linear combination of the mass and stiffness matrices, for suitable constants $\alpha$ and $\beta$.

*Systems with proportional viscous damping have exactly the same mode shapes as the corresponding undamped systems*. This is the key property.

The proof is quite simple. Inserting (10.61) into (10.56) and assuming, as usual, $\mathbf{w}_o(t) = \mathbf{x}\mathrm{e}^{\mu t}$, we get

$$(\mu^2 + \mu\alpha)\mathbf{M}\,\mathbf{x} + (\mu\beta + 1)\mathbf{K}\,\mathbf{x} = \mathbf{0} \tag{10.62}$$

that is

$$\left(\frac{\mu^2 + \mu\alpha}{\mu\beta + 1}\right)\mathbf{M}\,\mathbf{x} = -\mathbf{K}\,\mathbf{x} \tag{10.63}$$

With respect to the general case (10.60), we have only two matrices instead of three. And it makes quite a big difference in the physical behavior of the vehicle, as will be shown hereafter.

Now, letting

$$\lambda = \frac{\mu^2 + \mu\alpha}{\mu\beta + 1} \qquad \text{and} \qquad \mathbf{A} = -\mathbf{M}^{-1}\mathbf{K} \tag{10.64}$$

we end up with *exactly the same eigenvalue problem as the undamped system*

$$\mathbf{A}\,\mathbf{x} = \lambda\,\mathbf{x} \tag{10.65}$$

which provides two real eigenvalues $\lambda_1$ and $\lambda_2$, and the corresponding *real* eigenvectors $\mathbf{x}_1$ and $\mathbf{x}_2$.

Solving the first equation in (10.64) with $\lambda = \lambda_1$, we obtain $\mu_1$ and $\mu_3 = \bar{\mu}_1$. Similarly, solving with $\lambda = \lambda_2$ we obtain $\mu_2$ and $\mu_4 = \bar{\mu}_2$. Therefore, we have apparently four $\mu_j$ and only two eigenvectors $\mathbf{x}_j$. The point is that the eigenvectors have real components, and hence coincide with their complex conjugates. Strictly speaking, we have two couples of identical eigenvectors.

The general solution, that is the free oscillations, for proportional damping (and hence also for no damping, which is just a special case of proportional damping) is[3]

$$\mathbf{w}_o(t) = \mathbf{x}_1\left(\gamma_1\mathrm{e}^{\mu_1 t} + \gamma_3\mathrm{e}^{\mu_3 t}\right) + \mathbf{x}_2\left(\gamma_2\mathrm{e}^{\mu_2 t} + \gamma_4\mathrm{e}^{\mu_4 t}\right) \tag{10.66}$$

[3]The quarter car model is a two-degree-of-freedom system whose damping is certainly not proportional. It is worth comparing (10.66) with the more general (10.35).

Often, this equivalent expression, which only involves real quantities, is more convenient (cf. (6.226)

$$\mathbf{w}_o(t) = \chi_1 \mathbf{x}_1 \mathrm{e}^{-\zeta_1 \omega_1 t} \sin(\omega_{d_1} t + \varphi_1) + \chi_2 \mathbf{x}_2 \mathrm{e}^{-\zeta_2 \omega_2 t} \sin(\omega_{d_2} t + \varphi_2) \tag{10.67}$$

where

$$\mu_1 = -\zeta_1 \omega_1 + i\, \omega_{d_1} \quad \text{and} \quad \mu_2 = -\zeta_2 \omega_2 + i\, \omega_{d_2} \tag{10.68}$$

As usual in systems with proportional damping, $\zeta_j$ are the damping factors and $\omega_j$ are exactly the angular frequencies of the corresponding undamped system, while $\omega_{d_j} = \omega_j \sqrt{1 - \zeta_j^2}$ are the angular frequencies of the proportionally damped system.[4] The undamped system has $\lambda = \mu^2$, and hence

$$\omega_j = \sqrt{-\lambda_j} \quad \text{and} \quad \zeta_j = 0 \tag{10.69}$$

The four unknown constants depend on the four initial conditions.

The undamped and proportionally damped systems share almost everything, except the $\mu_j$'s. The really relevant aspect is that the eigenvectors $\mathbf{x}_j$ are exactly the same. This is the possible justification for "neglecting" the damping when studying the free oscillations of a vehicle. But the vehicle must be designed to have proportional damping, indeed. And a vehicle engineer should be well aware of this requirement.

### *10.6.3 Vehicle with Proportional Viscous Damping*

Looking at the three matrices (10.57), (10.58) and (10.59) for the case at hand, we see that the matrix $\mathbf{C}$ and the matrix $\mathbf{K}$ share the very same structure. Therefore, the only way to have proportional damping in a vehicle is to set $\alpha = 0$ and select springs and dampers such that

$$\beta = \frac{c_1}{k_1} = \frac{c_2}{k_2} \tag{10.70}$$

thus having in (10.61) $\mathbf{C} = \beta\, \mathbf{K}$. This can be done fairly easily and cheaply.

From (6.208) we obtain

$$\lambda_{1,2} = -\frac{1}{2 J_y m_s} \Big[ J_y(k_1 + k_2) + m_s(k_1 a_1^2 + k_2 a_2^2) \mp \sqrt{[J_y(k_1 + k_2) + m_s(k_1 a_1^2 + k_2 a_2^2)]^2 - 4 J_y m_s (a_1 + a_2)^2 k_1 k_2} \Big] \tag{10.71}$$

[4] The two natural frequencies of this model are not, of course, the two natural frequencies of the quarter car model. Another look at Fig. 10.3 should clarify the matter.

and the corresponding eigenvectors

$$\mathbf{x}_{1,2} = \left( \frac{1}{2(k_1 a_1 - k_2 a_2) m_s} \left[ J_y (k_1 + k_2) - m_s (k_1 a_1^2 + k_2 a_2^2) \mp \sqrt{[J_y (k_1 + k_2) + m_s (k_1 a_1^2 + k_2 a_2^2)]^2 - 4 J_y m_s (a_1 + a_2)^2 k_1 k_2} \right], \; 1 \right) \tag{10.72}$$

More compactly

$$\mathbf{x}_1 = (Z_{s_1}, 1) = \left( \frac{z_{s_1}(t)}{\theta_1(t)}, 1 \right) \qquad \text{and} \qquad \mathbf{x}_2 = (Z_{s_2}, 1) = \left( \frac{z_{s_2}(t)}{\theta_2(t)}, 1 \right) \tag{10.73}$$

which means that the free oscillations are the linear combination of the two natural modes

$$\begin{aligned} z_s(t) &= \chi_1 Z_{s_1} \mathrm{e}^{-\zeta_1 \omega_1 t} \sin(\omega_{d_1} t + \varphi_1) + \chi_2 Z_{s_2} \mathrm{e}^{-\zeta_2 \omega_2 t} \sin(\omega_{d_2} t + \varphi_2) = z_{s_1}(t) + z_{s_2}(t) \\ \theta(t) &= \chi_1 \mathrm{e}^{-\zeta_1 \omega_1 t} \sin(\omega_{d_1} t + \varphi_1) + \chi_2 \mathrm{e}^{-\zeta_2 \omega_2 t} \sin(\omega_{d_2} t + \varphi_2) = \theta_1(t) + \theta_2(t) \end{aligned} \tag{10.74}$$

The time histories for each mode are shown in Fig. 10.16. In each mode, the two coordinates move in a *synchronous way*. This is the key feature of systems with proportional damping.

Each natural mode is an oscillation around a point $P_i$ which has constantly zero vertical velocity. These points $P_1$ and $P_2$ are called *nodes* [5] and are defined as those points at which no vertical motion occurs when the system oscillates according to only one mode. Their position can be immediately obtained from (10.73). Each node $P_j$ is at a horizontal distance $d_j$ from $G_s$ equal to $Z_{s_j}$, taken in the positive direction if $Z_{s_j}$ is negative, and vice versa. In some sense, in a vehicle the eigenvectors can be visualized with a yardstick. This is not magic, it suffices to solve the equation

$$0 = \dot{z}_{s_j}(t) + d_j \dot{\theta}_j(t) \quad \Longrightarrow \quad d_j = -\frac{\dot{z}_{s_j}(t)}{\dot{\theta}_j(t)} = -\frac{z_{s_j}(t)}{\theta_j(t)} = Z_{s_j} \tag{10.75}$$

taking (10.73) into account.

The two natural modes and the corresponding nodes are shown in Fig. 10.17. Typically, the first mode, that is the one with lower natural frequency, has the node behind the rear axle. This mode is called *bounce*. The second mode has its node located ahead of $G_s$, near the front seat. This mode is called *pitch*.

We remark that fixed nodes are a prerogative of proportionally damped systems. More general systems still have two natural modes, but in each mode the two coordinates $z_{s_j}(t)$ and $\theta_j(t)$ are no longer equal to zero simultaneously, i.e., the motion

[5] Other common names are motion centers or oscillation centers.

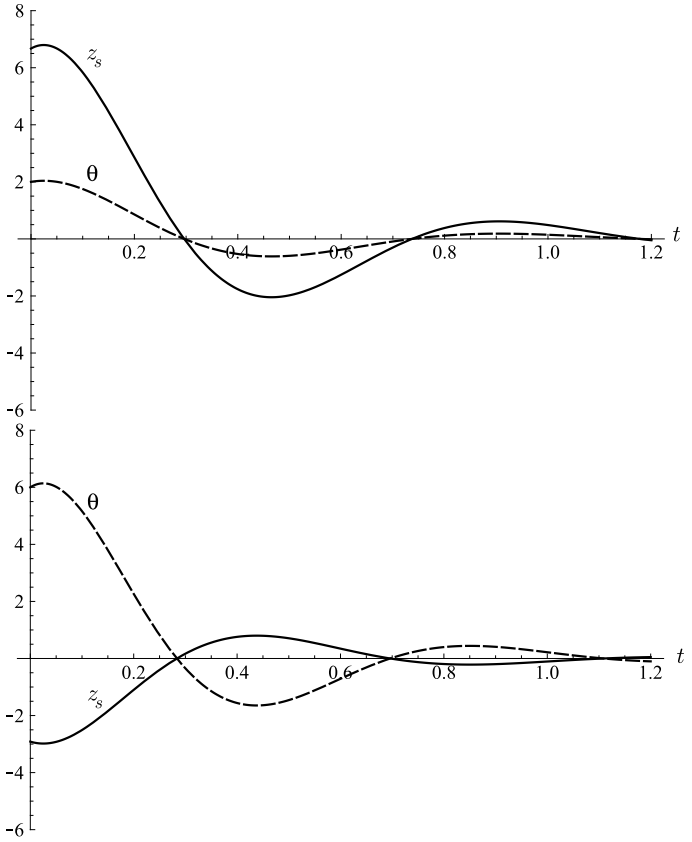


**Fig. 10.16** Time histories for bounce (top) and pitch (bottom) in case of proportional damping (synchronous motion)

is not synchronous. Therefore, their ratio $d_j(t)$ is a function of time and ranges from $-\infty$ to $+\infty$. At each time instant there is a different fixed point. We will discuss further this topic in Sect. 10.8.

### *10.6.4 Principal Coordinates*

In a vehicle with proportional damping, the nodes $P_1$ and $P_2$ also mark where the *principal coordinates* $z_b$ and $z_p$ are, as shown in Fig. 10.18.

Let $\mathbf{S}$ be the matrix whose columns are the two eigenvectors (10.73), that is

$$\mathbf{S} = \left[\mathbf{x}_1 | \mathbf{x}_2\right] \tag{10.76}$$

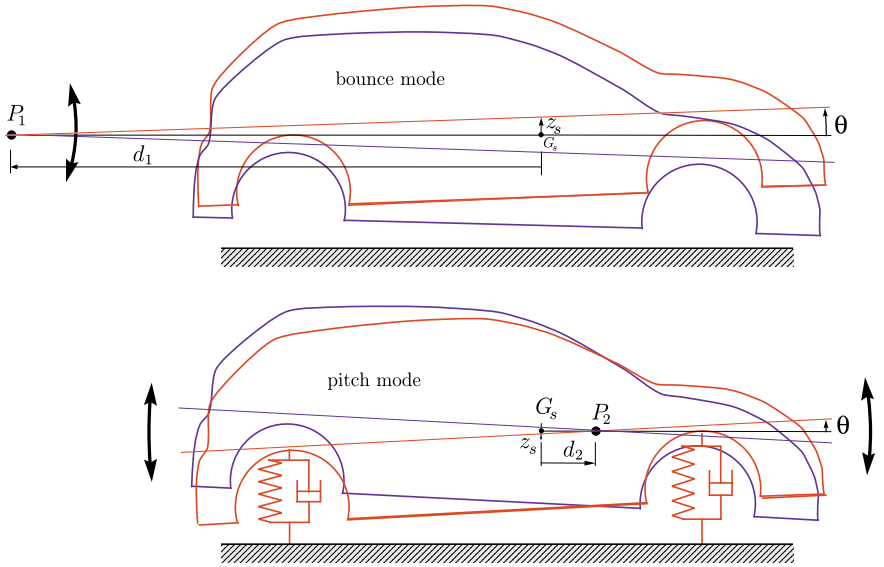


**Fig. 10.17** Fixed nodes $P_1$ and $P_2$ of the two natural modes in case of proportional damping

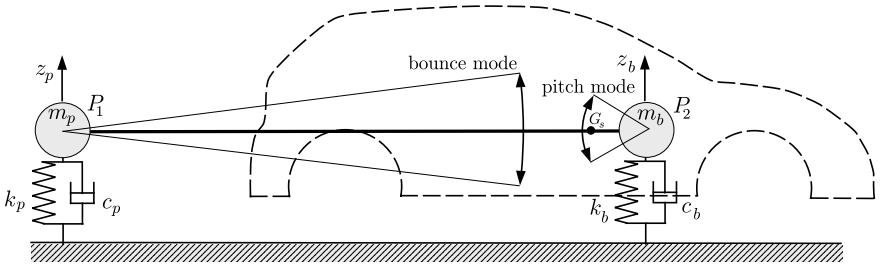


**Fig. 10.18** Principal coordinates and equivalent system (proportional damping)

The principal coordinates are equal to

$$\begin{bmatrix} z_b \\ z_p \end{bmatrix} = \mathbf{S}^{-1} \begin{bmatrix} z_s \\ \theta \end{bmatrix} \tag{10.77}$$

The key step is the diagonalization of the matrices. We have that

$$\begin{bmatrix} m_b & 0 \\ 0 & m_p \end{bmatrix} = \mathbf{S}^T \mathbf{M}\, \mathbf{S} \qquad \begin{bmatrix} c_b & 0 \\ 0 & c_p \end{bmatrix} = \mathbf{S}^T \mathbf{C}\, \mathbf{S} \qquad \begin{bmatrix} k_b & 0 \\ 0 & k_p \end{bmatrix} = \mathbf{S}^T \mathbf{K}\, \mathbf{S} \tag{10.78}$$

The system behaves precisely as if it were made up of two concentrated masses $m_b$ and $m_p$, each one with its own spring $k_b$ and $k_p$ and damper $c_b$ and $c_p$, respectively (Fig. 10.18). Obviously, we have that

$$\begin{aligned} 2\zeta_1\omega_1 &= \frac{c_b}{m_b} \qquad & \omega_1^2 &= \frac{k_b}{m_b} \\ 2\zeta_2\omega_2 &= \frac{c_p}{m_p} \qquad & \omega_2^2 &= \frac{k_p}{m_p} \end{aligned} \tag{10.79}$$

### 10.6.5 Selection of Front and Rear Suspension Vertical Stiffnesses

In case of proportional damping, the shape of both modes (and hence the position of both nodes) depends on two nondimensional parameters: $\rho$ and $\eta$.

The first parameter is the *dynamic index*

$$\rho = \frac{J_y}{m_s a_1 a_2} \tag{10.80}$$

It is a measure of how far the vehicle mass is distributed from its center of mass, with respect to the wheelbase. Of course, $\rho$ depends on the whole vehicle architecture and it is very difficult to modify it. Usually, in ordinary road cars $\rho$ ranges between 0.90 and 0.97 (Fig. 10.19). Cars with $\rho > 1$ must be like in Fig. 10.20, that is with the wheelbase much shorter than the whole vehicle length.

**Fig. 10.19** A modern car with $0.9 < \rho < 1$

**Fig. 10.20** An old car with $\rho > 1$

Another extremely important parameter is the ratio $\eta$

$$\eta = \frac{k_1\, a_1}{k_2\, a_2} \tag{10.81}$$

which characterizes how the axle stiffnesses relate to each other. Well tuned modern cars must have $\eta \simeq 0.95$.

Parameter $\eta$ has a simple physical meaning. Just look at it as

$$\eta = \frac{a_1/k_2}{a_2/k_1} \tag{10.82}$$

It is the ratio between the static deflection at the rear $mga_1/(lk_2)$ and the static deflection at the front $mga_2/(lk_1)$.[6]

For a deeper comprehension of the possible effects of these two parameters $\rho$ and $\eta$, we analyze the model of Fig. 10.15 in some special cases, before addressing how to tune the suspension stiffnesses in the general case.

For simplicity, we consider here the undamped system, whose governing equations are

$$\begin{aligned} m_s\, \ddot{z}_s + (k_1 + k_2)\, z_s + (k_1 a_1 - k_2 a_2)\, \theta &= 0 \\ J_y\, \ddot{\theta} + (k_1 a_1 - k_2 a_2)\, z_s + (k_1 a_1^2 + k_2 a_2^2)\, \theta &= 0 \end{aligned} \tag{10.83}$$

#### 10.6.5.1 Case 1: $\eta = 1$

If the suspension stiffnesses are selected such that $\eta = 1$, that is

$$k_1 a_1 = k_2 a_2 \tag{10.84}$$

the two equations in (10.83) become uncoupled. Both matrices are diagonal, which means that $z_s$ and $\theta$ are the principal coordinates. The two undamped natural angular frequencies are

$$\omega_1 = \sqrt{\frac{k_1 + k_2}{m_s}}, \qquad \omega_2 = \sqrt{\frac{k_1 a_1^2 + k_2 a_2^2}{J_y}} \tag{10.85}$$

Their ratio is equal, in this case, to the square root of the dynamic index

$$\left(\frac{\omega_1}{\omega_2}\right)^2 = \frac{J_y}{m_s a_1 a_2} = \rho \tag{10.86}$$

[6] Unfortunately, this physical interpretation often leads to the misconception that there are a front natural frequency and a rear natural frequency [6, p. 175].

The two eigenvalues are simply (cf. (10.72))

$$\mathbf{x}_1 = (1, 0) \quad \text{and} \quad \mathbf{x}_2 = (0, 1) \tag{10.87}$$

Therefore, the bounce mode is a pure vertical translation and the pitch mode is a rotation around $G_s = P_2$.

#### 10.6.5.2 Case 2: $\rho = 1$

Now, let us assume that a vehicle has $\rho = 1$, that is

$$J_y = m a_1 a_2 \tag{10.88}$$

In this case the two principal coordinates are the vertical displacements $z_1$ and $z_2$ given in (10.2) and in Fig. 10.15, that is the displacements of the vehicle body at the two axles. After a little algebra, it is possible to rewrite the governing equations as

$$\begin{aligned} m_{s_1} \ddot{z}_1 + k_1 z_1 &= 0, \\ m_{s_2} \ddot{z}_2 + k_2 z_2 &= 0, \end{aligned} \tag{10.89}$$

where

$$m_{s_1} = m_s \frac{a_2}{a_1 + a_2} \qquad m_{s_2} = m_s \frac{a_1}{a_1 + a_2} \tag{10.90}$$

The undamped natural frequencies are

$$\omega_1 = \sqrt{\frac{k_1}{m_{s_1}}} \qquad \omega_2 = \sqrt{\frac{k_2}{m_{s_2}}} \tag{10.91}$$

Their ratio is, in this case, equal to the square root of $\eta$

$$\left(\frac{\omega_1}{\omega_2}\right)^2 = \frac{k_1 a_1}{k_2 a_2} = \eta \tag{10.92}$$

The two eigenvectors in the original coordinates $z_s$ and $\theta$ are (cf. (10.72))

$$\mathbf{x}_1 = (a_2, 1) \quad \text{and} \quad \mathbf{x}_2 = (-a_1, 1) \tag{10.93}$$

The nodes are precisely over the front axle and the rear axle, as expected. Otherwise, $z_1$ and $z_2$ would not be the principal coordinates.

#### 10.6.5.3 Case 3: $\eta = 1$ and $\rho = 1$

But what happens if we set both $\eta$ and $\rho$ equal to one? From (10.86) and (10.92) we obtain that

$$\left(\frac{\omega_1}{\omega_2}\right)^2 = 1 \tag{10.94}$$

that is the two undamped modes have exactly the same natural frequency.

The analysis of the shape of the two modes is more tricky. Apparently there is a paradox: the modes obtained before for $\eta = 1$ are not consistent with those obtained for $\rho = 1$, and vice versa. Which prevails? There is only one way out. Any point can be a node, that is, any vector $\mathbf{x}$ is an eigenvector. This happens because the matrix $\mathbf{A} = -\mathbf{M}^{-1}\mathbf{K}$ is like the identity matrix $\mathbf{I}$, times a suitable constant.

A vehicle designed to have $\eta = \rho = 1$ would have a very unpredictable behavior. As a matter of fact, a real vehicle could fulfill this condition only approximately. Therefore, the two nodes would be quite randomly located. Certainly, not a desirable behavior.

## 10.7 Tuning of Suspension Stiffnesses

So far we have obtained the following results about the vehicle free oscillations:

1. tires can be considered as rigid;
2. damping should be proportional to the corresponding stiffness;
3. the two natural frequencies of the undamped system are very close to the natural frequencies of the proportionally damped system;
4. the shape of the modes of the undamped system are exactly equal to the shape of the modes of the proportionally damped system.

Now we can proceed to discus how to choose $k_1$ and $k_2$. There are basically two requirements for road cars:

- both natural frequencies must fall in the range 1.0–1.5 Hz;
- the pitch mode should have its node located at about the front seat.

The first rule comes from the observation that oscillations at 1.0–1.5 Hz are quite comfortable for human beings. The second rule is an attempt to reduce the pitch motion of the driver. Pitch is typically more annoying than bounce.

As already stated, the value of $\rho$ cannot be modified, unless the vehicle is completely redesigned. Modern road cars have (Fig. 10.19)

$$\rho \simeq 0.95 \tag{10.95}$$

To locate the pitch node on the front seat we can act on $\eta$, that is on the relative stiffnesses. Usually, a good value is

$$\eta \simeq 0.95 \tag{10.96}$$

With both $\eta$ and $\rho$ slightly lower than one, and with proportional damping, the car damped oscillations are like in Fig. 10.17, with the pitch node near the front seat and the bounce node quite far away behind the car. This is usually acknowledged as comfortable behavior.

For completeness, we provide the general formulæ to compute the horizontal distances $d_i$ from $G_s$ of the nodes of bounce and pitch (Fig. 10.17), as functions of $\eta$ and $\rho$

$$d_i = (a_1 + a_2)\frac{\rho - \eta + (\eta - 1)(\rho + 1)\chi \pm \sqrt{[(\eta - 1)(\rho - 1)\chi + \eta + \rho]^2 - 4\eta\rho}}{2(\eta - 1)} \tag{10.97}$$

where $\chi = a_2/(a_1 + a_2)$. Positive values of $d_i$ means toward the rear axle, and viceversa.

### 10.7.1 Optimality of Proportional Damping

Summing up, for a good suspension design we have found that we should fulfill these requirements

- $c_j \simeq c_{\text{opt}}$;
- $c_1/k_1 = c_2/k_2$ (proportional damping);
- $\eta \simeq 0.95$ (if also $\rho \simeq 0.95$).

But do they conflict with each other or not? Let us develop this point.

Optimal damping requires (cf. (10.43))

$$c_1 \simeq \sqrt{\frac{m_{s_1} k_1}{2}} \quad \text{and} \quad c_2 \simeq \sqrt{\frac{m_{s_2} k_2}{2}} \tag{10.98}$$

where $m_{s_1} = m_s a_2/l$ and $m_{s_2} = m_s a_1/l$. At the same time, proportional damping requires $c_1/k_1 = c_2/k_2 = \beta$, which combined with the former expression means

$$\sqrt{\frac{m_{s_1} k_1}{2}}\frac{1}{k_1} \simeq \sqrt{\frac{m_{s_2} k_2}{2}}\frac{1}{k_2} \tag{10.99}$$

that is

$$\sqrt{\frac{m_s a_2}{k_1}} \simeq \sqrt{\frac{m_s a_1}{k_2}} \quad \Longrightarrow \quad k_1 a_1 \simeq k_2 a_2 \quad \Longrightarrow \quad \eta \simeq 1 \tag{10.100}$$

Therefore, we see that these three requirements do not conflict with each other.

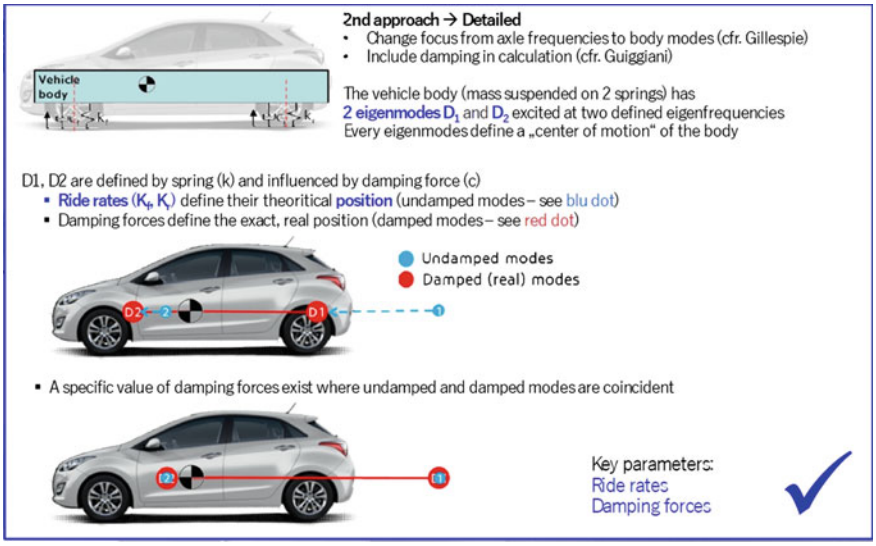


**Fig. 10.21** Industrial application of proportional damping

We have insisted many times about having a vehicle with springs and dampers tuned to have proportional damping. The importance of this feature has been confirmed by Hyundai Motor Europe Technical Center GmbH in the communication entitled "A new R&H evaluation methodology applied during Hyundai i30 development", presented by Antonino Pizzuto at 2017 VI-grade Users Conference (Fig. 10.21).

As shown in Fig. 10.17, fixed nodes are a prerogative of proportionally damped systems. This is the outcome of having synchronous motion of both degrees of freedom in each natural mode, as shown in Fig. 10.16.

### *10.7.2 A Numerical Example*

Crunching numbers helps a lot to grasp what we are really doing.

Let a vehicle have these features:

- sprung mass $m_s = 1000\,\text{kg}$ and moment of inertia $J_y = 1620\,\text{kgm}^2$;
- $a_1 = 1.2\,\text{m}$ and $a_2 = 1.5\,\text{m}$;
- axle vertical stiffnesses $k_1 = 31500\,\text{N/m}$ and $k_2 = 28000\,\text{N/m}$;
- proportional damping with $\beta = c_1/k_1 = c_2/k_2 = 0.0936\,\text{s}$.

We obtain immediately the dynamic index

$$\rho = \frac{J_y}{m_s a_1 a_2} = \frac{1620}{1800} = 0.9 \tag{10.101}$$

and the ratio

$$\eta = \frac{k_1 a_1}{k_2 a_2} = \frac{31.5 \times 1.2}{28.0 \times 1.5} = 0.9. \tag{10.102}$$

Both $\rho$ and $\eta$ are lower than one, although $k_1 > k_2$.

The matrix $A$ is

$$\mathbf{A} = -\begin{bmatrix} 59.5 & -4.2 \\ -2.592 & 66.89 \end{bmatrix} \tag{10.103}$$

with eigenvalues

$$\lambda_1 = -58.24 \text{ s}^{-2} \qquad \lambda_2 = -68.15 \text{ s}^{-2} \tag{10.104}$$

and eigenvectors

$$\mathbf{x}_1 = (3.336, 1) \qquad \mathbf{x}_2 = (-0.486, 1) \tag{10.105}$$

The bounce mode has its node 3.336 m behind $G_s$, and hence $3.33 - 1.50 = 1.83$ m behind the rear axle (Fig. 10.17). The pitch mode has its node 0.486 m ahead of $G_s$.

Should the system be undamped, the natural frequencies would be

$$f_1 = \frac{\sqrt{-\lambda_1}}{2\pi} = 1.21 \text{ Hz} \qquad f_2 = \frac{\sqrt{-\lambda_2}}{2\pi} = 1.31 \text{ Hz} \tag{10.106}$$

These frequencies could be estimated by means of the simple formulæ (10.85). The approximate values are $f_1 \simeq 1.23$ Hz and $f_2 \simeq 1.30$ Hz, quite close to the exact ones although $\eta \neq 1$.

With proportional damping, we have to solve (10.64)

$$\mu^2 - \beta \lambda_i \mu - \lambda_i = 0 \tag{10.107}$$

with $\beta = c_1/k_1 = c_2/k_2 = 0.0936$ s, thus getting

$$\mu_{1,3} = -2.73458 \pm i\, 7.12481 \text{ s}^{-1} \qquad \mu_{2,4} = -3.19975 \pm i\, 7.60983 \text{ s}^{-1} \tag{10.108}$$

From the imaginary part we obtain the natural frequencies of the damped system

$$f_{s1} = \frac{\text{Im}(\mu_1)}{2\pi} = 1.13 \text{ Hz} \qquad f_{s2} = \frac{\text{Im}(\mu_3)}{2\pi} = 1.21 \text{ Hz} \tag{10.109}$$

They are about 10% lower than those of the undamped system. Both fall within the acceptable range.

The bounce and pitch modes have $\zeta_1 = 0.36$ and $\zeta_2 = 0.39$, respectively. There is quite a lot of damping indeed.

If, just to see what happens, we set $J_y = 1980\,\text{kgm}^2$, thus having $\rho = 1.1$, we get that the bounce mode has $f_1 = 1.24$ Hz and its node located 2.93 m ahead of $G_s$,

while the pitch mode has $f_2 = 1.16$ Hz and its node located at 0.67 m behind $G_s$. As expected, many things have been inverted, like the node positions and the frequency order.

## 10.8 Non-proportional Damping

A vehicle with non-proportional damping has, in each natural mode, non-synchronous motion of the two degrees of freedom, as shown in Fig. 10.22, where the front damping coefficient has been reduced by 10%, while the rear damping coefficient has been increased by 10%. Also shown in Fig. 10.22 are the plots of $d_1(t)$ and $d_2(t)$, that is the time-varying positions of the nodes w.r.t. $G_s$

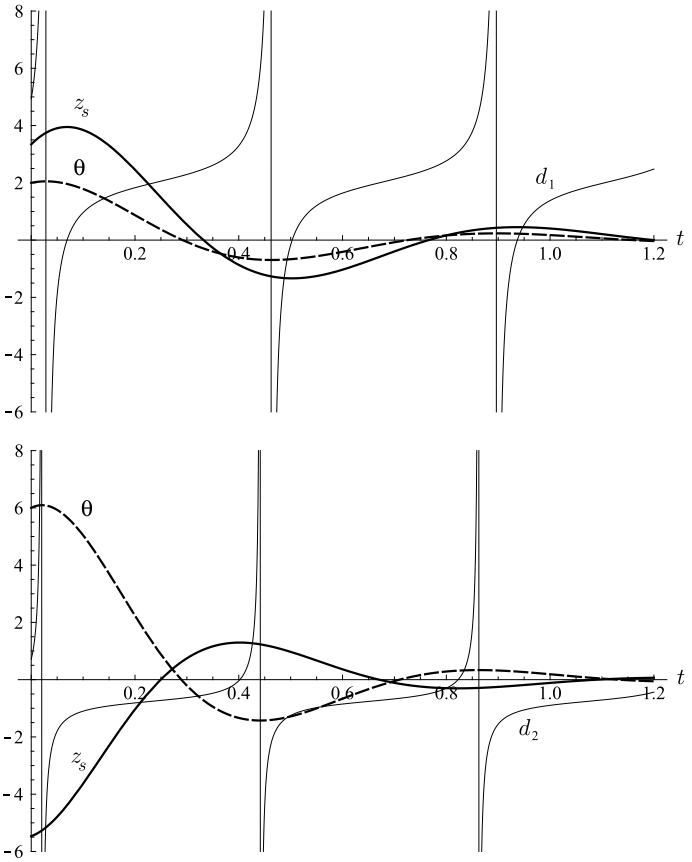


**Fig. 10.22** Time histories for bounce (top) and pitch (bottom) in case of non-proportional damping (non-synchronous motion)

$$0 = \dot{z}_{s_j}(t) + d_j(t)\dot{\theta}_j(t) \quad \Longrightarrow \quad d_j(t) = -\frac{\dot{z}_{s_j}(t)}{\dot{\theta}_j(t)} \tag{10.110}$$

These positions are functions of time and cycle from zero (when $\dot{z}_s = 0$) to $\pm\infty$ (when $\dot{\theta} = 0$). Therefore, the vehicle still has two modes, but their shapes are somehow mixed up. They are not so neatly different as they are with proportional damping. It is no longer possible to define the principal coordinates.

Actually, in some sense, both modes share some fundamental features. In both modes there are time instants in which $\dot{z}_s = 0$ with $\dot{\theta} \neq 0$, and hence the vehicle body is rotating around $G_s$, and other time instants in which $\dot{\theta} = 0$ with $\dot{z} \neq 0$, and hence the vehicle body is having a pure vertical translation.

Also observe that, differently from (10.75), the ratio in (10.110) do not extend to the ratio of coordinates.

## 10.9 Interconnected Suspensions

So far we have employed the model of Fig. 10.15. Implicitly, we have considered it to be quite a general model for studying the ride of a two-axle vehicle. But it is not. Let us address the problem from a fresh point of view.

Still using $z_s$ and $\theta$ as coordinates, a more general form of the equations of motion (10.83) for a linear two-degree-of-freedom undamped system are

$$\begin{aligned} m_s\,\ddot{z}_s + k_{zz}\,z_s + k_{z\theta}\,\theta &= 0 \\ J_y\,\ddot{\theta} + k_{\theta z}\,z_s + k_{\theta\theta}\,\theta &= 0 \end{aligned} \tag{10.111}$$

where $k_{z\theta} = k_{\theta z}$.

Each stiffness has a clear physical meaning. Let us impose a pure translation $z_s$ to the system, that is with $\theta = 0$. The system reacts with a force $-k_{zz}\,z_s$ and a couple $-k_{\theta z}\,z_s$. Similarly, imposing a pure rotation around $G_s$, the system reacts with a force $-k_{z\theta}\,\theta$ and a couple $-k_{\theta\theta}\,\theta$.

In general, any $2 \times 2$ stiffness matrix is characterized by three coefficients. But in the system of Fig. 10.15 we have only two parameters, namely $k_1$ and $k_2$. Therefore the following equations

$$\begin{aligned} k_1 + k_2 &= k_{zz} \\ k_1 a_1 - k_2 a_2 &= k_{z\theta} \\ k_1 a_1^2 + k_2 a_2^2 &= k_{\theta\theta} \end{aligned} \tag{10.112}$$

may not all be fulfilled. As anticipated, the scheme of Fig. 10.15 is not as general as it may seem at first. We need a suspension layout with three springs, although we still have only two axles.

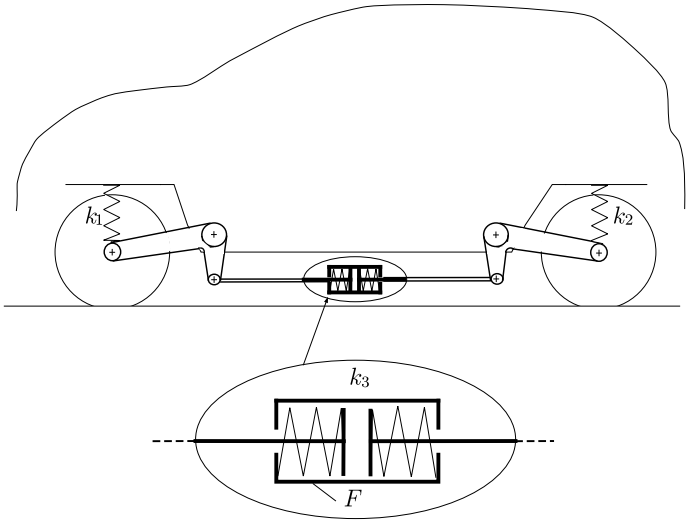


**Fig. 10.23** Schematic for interconnected suspensions

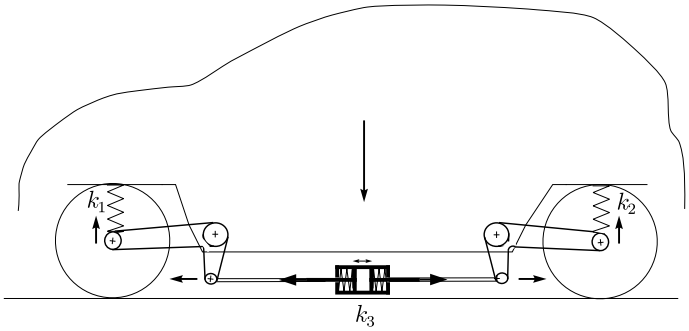


**Fig. 10.24** Interconnected suspensions activated when bouncing

*Interconnected suspensions* are the solution to this apparent paradox. A very basic scheme of interconnected suspensions is shown in Fig. 10.23. Its goal is to explain the concept, not to be a solution to be adopted in real cars (although, it was actually employed many years ago).

To understand how it works, first suppose the car bounces, as in Fig. 10.24. The springs contained in the floating device $F$ get compressed, thus stiffening both axles. On the other hand, if the car pitches, as in Fig. 10.25, the floating device $F$ just translates longitudinally, without affecting the suspension stiffnesses. This way we have introduced the third independent spring $k_3$ in our vehicle.

Obviously, hydraulic interconnections are much more effective, but the principle is the same. We have an additional parameter to tune the vehicle oscillatory behavior.

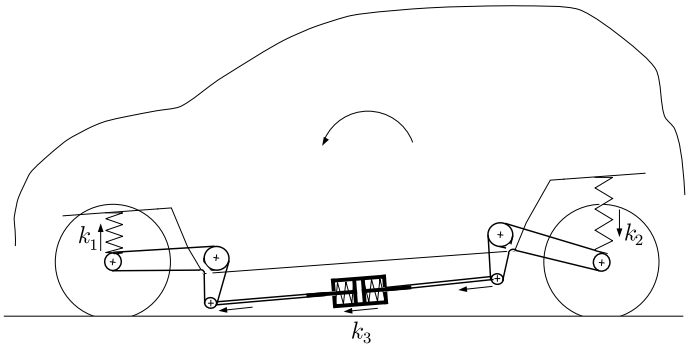


**Fig. 10.25** Interconnected suspensions not activated when pitching

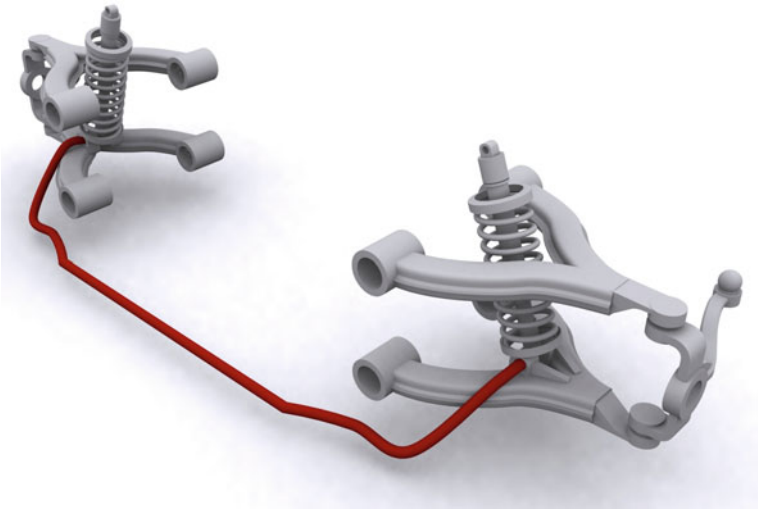

**Fig. 10.26** Transversal interconnection by means of the anti-roll bar [7]

Although only a few cars have longitudinal interconnection, almost all cars are equipped with torsion (anti-roll) bars, and hence they have transversal interconnection. An example is shown in Fig. 10.26.

Using interconnected suspensions may lead to non-proportional damping, if proper counteractions are not taken, that is if the floating device $F$ adds a stiffness $k_3$ without also adding a damping coefficient $c_3$.

## 10.10 Exercises

### *10.10.1 Playing with η*

*By means of* (10.97) *it is fairly easy to locate the nodes of bounce and pitch modes, in a vehicle with damping proportional to stiffness. Assuming* $a_1 + a_2 = 2.6\,\text{m}$ *and* $\chi = a_2/(a_1 + a_2) = 0.5$*, find* $d_1$ *and* $d_2$ *in the following cases:*

1. $\eta = 0.95$, $\rho = 0.95$;
2. $\eta = 0.99$, $\rho = 0.95$;
3. $\eta = 0.9$, $\rho = 0.95$;
4. $\eta = 0.6$, $\rho = 0.95$;
5. $\eta = 0.3$, $\rho = 0.95$.

*Before jumping at the solution, try to figure out what the outcome can be.*

**Solution**

To visualize and understand the results it is recommended to refer to Fig. 10.17

1. $d_1 = 3.06\,\text{m}$, $d_2 = -0.52\,\text{m}$;
2. $d_1 = 13.06\,\text{m}$, $d_2 = -0.12\,\text{m}$;
3. $d_1 = 2.03\,\text{m}$, $d_2 = -0.79\,\text{m}$;
4. $d_1 = 1.40\,\text{m}$, $d_2 = -1.14\,\text{m}$;
5. $d_1 = 1.33\,\text{m}$, $d_2 = -1.21\,\text{m}$.

### *10.10.2 Playing with ρ*

*By means of* (10.97) *it is fairly easy to locate the nodes of bounce and pitch modes, in a vehicle with damping proportional to stiffness. Assuming* $a_1 + a_2 = 2.6\,\text{m}$ *and* $\chi = a_2/(a_1 + a_2) = 0.5$*, find* $d_1$ *and* $d_2$ *in the following cases:*

1. $\eta = 0.95$, $\rho = 0.95$;
2. $\eta = 0.95$, $\rho = 0.9$;
3. $\eta = 0.95$, $\rho = 0.8$;
4. $\eta = 0.95$, $\rho = 1$;
5. $\eta = 0.95$, $\rho = 1.1$;
6. $\eta = 1.1$, $\rho = 1.1$.

*Before jumping at the solution, try to figure out what the outcome can be.*

**Solution**

To visualize and understand the results it is recommended to refer to Fig. 10.17

1. $d_1 = 3.06\,\text{m}$, $d_2 = -0.52\,\text{m}$;
2. $d_1 = 5.35\,\text{m}$, $d_2 = -0.28\,\text{m}$;

3. $d_1 = 10.27\,\text{m}$, $d_2 = -0.13\,\text{m}$;
4. $d_1 = 1.3\,\text{m}$, $d_2 = -1.3\,\text{m}$;
5. $d_1 = 0.34\,\text{m}$, $d_2 = -5.41\,\text{m}$;
6. $d_1 = 3.29\,\text{m}$, $d_2 = -0.56\,\text{m}$.

Quite interesting the comparison between the first and the last cases.

## 10.11 Summary

In this chapter, the ride behavior of vehicles has been investigated. To keep the analysis very simple, two two-degree-of-freedom models have been formulated. The first, called quarter car model, has been used for determining the right amount of damping to have good comfort and/or road holding when the vehicle travels on a bumpy road (forced oscillations). In this framework, the inerter has been also introduced and discussed.

Free oscillations have been studied assuming the tires are perfectly rigid. The importance of proportional damping has been highlighted. This analysis has given indications on how to select spring stiffnesses.

Interconnected suspensions have been mentioned to show how to have a very general stiffness matrix.

## 10.12 List of Some Relevant Concepts

p. 418 — the inerter is a device that provides a force proportional to the relative acceleration between its attachment points;
p. 423 — the quarter car model is mainly used to study the vibrational behavior of a vehicle travelling on an uneven road;
p. 426 — the inertance acts as a spring softener at high frequencies;
p. 429 — the quarter car model is a tool for the selection of the damping coefficient of the dampers;
p. 440 — systems with proportional viscous damping have exactly the same mode shapes as the corresponding undamped systems;
p. 443 — only vehicles with proportional viscous damping have simple bounce and pitch modes.

## 10.13 Key Symbols

| | |
|---|---|
| $a_1$ | distance of $G$ from the front axle |
| $a_2$ | distance of $G$ from the rear axle |

| | |
|---|---|
| $b$ | inertance |
| $c$ | damping coefficient |
| $\mathbf{C}$ | damping matrix |
| $c_i$ | damping coefficient |
| $c_{\text{opt}}$ | optimal damping |
| $f$ | frequency (Hz) |
| $G$ | center of mass |
| $h$ | vertical displacement |
| $H$ | amplitude of the excitation |
| $i$ | imaginary unit |
| $l$ | wheelbase |
| $J_y$ | moment of inertia |
| $k$ | stiffness |
| $\mathbf{K}$ | stiffness matrix |
| $k_i$ | stiffness |
| $\mathbf{M}$ | mass matrix |
| $m_n$ | unsprung mass |
| $m_s$ | sprung mass |
| $N$ | amplitude of the vertical load on the tire |
| $p$ | tire vertical stiffness |
| $x$ | coordinate |
| $\mathbf{x}$ | eigenvector |
| $y$ | coordinate |
| $Y$ | amplitude (real) |
| $\mathsf{Y}$ | amplitude (complex) |
| $z$ | coordinate |
| $z_b$ | principal coordinate (bounce) |
| $z_p$ | principal coordinate (pitch) |
| $z_s$ | vertical coordinate of $G$ |
| $Z$ | amplitude (real) |
| $\mathsf{Z}$ | amplitude (complex) |

| | |
|---|---|
| $\alpha$ | coefficient |
| $\beta$ | coefficient |
| $\gamma_i$ | coefficient |
| $\zeta_i$ | damping ratio |
| $\eta$ | $k_1 a_1/(k_2 a_2)$ |
| $\theta$ | pitch rotation |
| $\lambda$ | eigenvalue |
| $\mu$ | complex exponent |
| $\rho$ | dynamic index |
| $\omega_i$ | natural angular frequency |
| $\omega_{d_i}$ | natural angular frequency of the damped system |
| $\Omega$ | angular frequency of the excitation |

## References

1. Bastow D, Howard G, Whitehead JP (2004) Car suspension and handling, 4th edn. SAE International, Warrendale.
2. Bourcier de Carbon C (1950) Theorie mathématique et réalisation pratique de la suspension amortie des véhicules terrestres. In: 3rd Congres Technique de l'Automobile, Paris
3. Dixon JC (1991) Tyres, suspension and handling. Cambridge University Press, Cambridge.
4. Dixon JC (2009) Suspension geometry and computation. Wiley, Chichester.
5. Font Mezquita J, Dols Ruiz JF (2006) La Dinámica del Automóvil. Editorial de la UPV, Valencia.
6. Gillespie TD (1992) Fundamentals of vehicle dynamics. SAE International, Warrendale.
7. Longhurst C (2013). www.carbibles.com
8. Palm III WJ (2007) Mechanical vibration. Wiley, New York
9. Popp K, Schiehlen W (2010) Ground vehicle dynamics. Springer, Berlin.
10. Smith MC (2002) Synthesis of mechanical networks: the inerter. IEEE Trans Autom Control 47:1648–1662.
11. Wong JY (2001) Theory of ground vehicles. Wiley, New York.